An open-ocean forcing in the East China and Yellow seas

Chao Ma,[1] Dexing Wu,[1] Xiaopei Lin,[1] Jiayan Yang,[2] and Xia Ju[3]

Received 11 February 2010; revised 25 August 2010; accepted 1 September 2010; published 21 December 2010.

[1] Recent studies have demonstrated that the annual mean barotropic currents over the East China and Yellow seas (ECYS) are forced primarily by the oceanic circulation in the open-ocean basin through the Kuroshio Current (KC), the western boundary current of the subtropical gyre in the North Pacific Ocean. The local wind stress forcing plays an important but secondary role. Those previous results were mainly qualitative and from a simple barotropic model forced by a steady wind stress field. They remain to be tested in a more complete 3-D model with both wind stress and buoyancy fluxes. In addition, the seasonal variability of major ECYS currents may involve different forcing mechanisms than their annually averaged fields do, and this can only be addressed when a seasonally varying forcing is used in the model. In this paper, we will address these issues by using a 3-D baroclinic model. Our results confirm the finding from the previous studies that the KC is the primary forcing mechanism for major annually mean currents in the ECYS, which include the Taiwan Strait Current, the Tsushima Warm Current, and the Yellow Sea Warm Current (YSWC), etc. However, the local monsoonal forcing plays a prominent role in modulating the seasonal variability of all major currents in the region. A deep northwestward intrusion of the YSWC in winter, for instance, is mainly due to a robustly developed China Coastal Current and Korea Coastal Current, which draw water along the Yellow Sea Trough to feed the southward flows along the west and east coasts of the Yellow Sea.

Citation: Ma, C., D. Wu, X. Lin, J. Yang, and X. Ju (2010), An open-ocean forcing in the East China and Yellow seas, *J. Geophys. Res.*, *115*, C12056, doi:10.1029/2010JC006179.

1. Introduction

[2] The East Asian Marginal Seas consist of some semi-enclosed deep basins, such as the South China Sea (SCS) and the Japan/East Sea (JES), and shallow shelves like the East China and Yellow seas (ECYS). This study focuses some major currents in the ECYS between the Taiwan and Tsushima Straits. The flow along the eastern Taiwan Strait, though varies seasonally in strength, is believed to be perennially northward [*Fang et al.*, 1991; *Su et al.*, 1994; *Isobe*, 1999; *Wang et al.*, 2003; *Zhu et al.*, 2004]. The surface wind is dominated by the East Asian Monsoon, and thus changes seasonally from a robust northeasterly in the winter to a mild southwesterly during the summer. The annually averaged wind stress is decisively northeasterly (southwestward) with a magnitude on the order of 1 dyn cm^{-2}. Therefore, the annually averaged Taiwan Strait Current (TSC) is a counter-wind current against the prevailing southwestward wind stress [*Guan and Fang*, 2006].

[3] Under this seasonally reversing monsoonal forcing, the water masses from both the East China Sea (ECS) and the SCS could enter the strait. The subsequent mixture of the two water masses and a possible direct intrusion from the Kuroshio Current (KC) can further complicate the characteristics of the hydrographic structure within the strait. The consensus is that the transport is northeastward during the southwesterly monsoon. The flow in the winter is more debatable. The majority view is that the winter flow is weakly northeastward at least on the eastern side of the strait (see a recent review by *Guan and Fang* [2006]). Nevertheless, it has been well accepted that the annually averaged flow is northward despite that the annually averaged wind stress is strongly southwestward. Here we will review briefly some previous results. *Guan* [1986] provided an observation-based description of the flow along the Taiwan Strait and some evidences for the northward flow in winter. On the basis of velocity observations from fixed stations, *Fang et al.* [1991] calculated volume transport through the Taiwan Strait, and found the average in the winter half-year is about 1.0 Sv while in summer half-year is about 3.1 Sv, and the annual mean is 2 Sv (the positive value refers to a northeastward transport). *Teague et al.* [2003] calculated that the average transport was 0.14 Sv from October to December 1999 using the profiled current data from bottom-mounted Acoustic Doppler Current Profiler (ADCP) stations. *Wang et al.* [2003] calculated the average transport

[1]Physical Oceanography Laboratory, Ocean University of China, Qingdao, China.
[2]Department of Physical Oceanography, Woods Hole Oceanographic Institution, Woods Hole, Massachusetts, USA.
[3]The First Institute of Oceanography, State Oceanic Administration, Qingdao, China.

0148-0227/10/2010JC006179

was 1.8 Sv between 1999 and 2001, by using ship-mounted ADCP data. The existence of the perennially northward TSC has also been simulated by various models. For instance, *Guo* [1999] used the Princeton Ocean Model (POM) and simulated a TSC which varies seasonally from 1 Sv in winter to 3 Sv in summer and has an annually averaged transport of 1.9 Sv. His result was quite consistent with the observationally based estimate by *Fang et al.* [1991]. More recently *Fang et al.* [2002] used the Modular Ocean Model 2 (MOM2) and simulated an annual cycle of TSC transport from −0.36 Sv in November to 2.87 Sv in July with a yearly averaged transport of 1.15 Sv. The model result indicates that the observation of 0.14 Sv by *Teague et al.* [2003] for the period from October to December 1999 was made during the weakest TSC season.

[4] So far, the mechanism of the winter counter-wind currents off the southeastern China coast has not been totally solved, though a number of studies have been done in the past decades. *Chuang* [1985] concluded that the current in the Taiwan Strait was driven by the sea surface slope and wind stress. Soon thereafter, he believed that this sea surface slope was induced by the KC branching to the SCS through the Luzon Strait [*Chuang*, 1986]. *Su and Wang* [1987] adopted a barotropic model with ideal coastline and found that there is no flow entering the Taiwan Strait directly from the Kuroshio SCS branch, instead of a cyclonic gyre in the SCS, at which northwest corner there is a component flowing over the continental slope. Water trapped by the shelf break topography was guided to flow northward into the Taiwan Strait and eventually to flow into the ECS. *Li et al.* [1992, 1993] indicated that the northward flow in winter in the Taiwan Strait mainly originates from the South China Sea Warm Current, rather than directly from the Kuroshio branch south of Taiwan. *Li et al.* [1993] and *Li and Zeng* [1994] proposed that the effects of the factors such as wind, bottom topography, coastal configuration as well as the Kuroshio intrusion are all able to produce the South China Sea Warm Current, but the Kuroshio intrusion is not the determinant for the formation of it. Recently, *Guan and Fang* [2006] reviewed the winter counter-wind currents off the southeastern China coast.

[5] For an along-bathymetry flow through a narrow strait, the cross-channel component of the velocity is typically small, and thus, the leading dynamic balance in the along-strait direction is between the pressure gradient, wind stress, and friction. The friction, in general, is to retard the flow, and thus is not considered as a driver for the flow. The wind stress, in the TSC case, is against the flow on the annually averaged sense and thus is unlikely the direct driver for the counter-wind current. So the most likely driver for the TSC is the pressure difference between the southern and northern strait and this has been well recognized in many previous studies [*Chuang*, 1985; *Fang*, 1995; *Su*, 2001]. There have been two different views regarding what sets and maintains this pressure difference. One suggested that the TSC is thermally driven. *Fang and Zhao* [1988] found that the steric height at the sea surface around the Luzon Strait is higher than the height in the area to the east of the Tsugaru and Soya Straits. They also proposed that the sea surface slope along the southeast coast of China is related to the high sea level in the western tropical Pacific through the Luzon Strait, and the large difference of the sea level along the western boundary of the ocean is mainly a result of the thermohaline effect [*Fang and Zhao*, 1988; *Fang et al.*, 1991]. The effect of the Kuroshio branching on the sea surface slope is considered as a secondary factor [*Fang et al.*, 1992]. Another group of studies related it to the entire low-latitude western boundary current. *Minato and Kimura* [1980] first considered the sea level variation along the western boundary of the ocean on the basis of wind-driven ocean circulation model. *Fang* [1995] proposed that, owing to the variation of the Coriolis parameter with latitude, the sea level difference between the two sides of the western boundary current is larger in the south than in the north. Since the sea level is identical along the east side of the KC, the sea level along the west side is higher in the south than in the north.

[6] On the other hand, *Yang* [2007] hypothesized that the KC through its interaction with Taiwan Island is primarily responsible for setting this pressure gradient. In another study, *Yang* [2006] proposed that the Tsushima Warm Current (TsWC) induces flows (in the form of source- and sink-driven currents) along isobaths over the ECYS and makes an important secondary contribution to the northward transport across the Taiwan Strait.

[7] There are two major objectives of this study: (1) to test the KC forcing mechanism of *Yang* [2007] in a three-dimensional model and (2) to examine the mechanism(s) for seasonal variability in the ECYS. The first objective is motivated by some previous studies [e.g., *Isobe*, 2000] that showed that baroclinic processes are important for the intrusion of KC into the shelf. So the barotropic model results from *Yang* [2007] need to be tested in a more complete three-dimensional model. The second objective is a natural follow up of the first one. Although the KC varies seasonally, the magnitude of its seasonal variability is considerably less than the annually mean transport [*Guan*, 1981; *Johns et al.*, 2001; *Liang et al.*, 2003]. The seasonal variation of the TSC as relative to the mean transport, however, is much larger and thus the KC forcing alone would be difficult to explain the large seasonal variability of the TSC and other major currents in the ECYS. So the local monsoonal forcing could be important in modulating the seasonal cycles.

[8] In this paper, we will use a three-dimensional ocean model to examine both KC and monsoon forcing in the Taiwan Strait and over a broader ECYS region. The standard run is a baroclinic model with full forcing, which includes buoyancy fluxes, wind stress and boundary inflow. Several sensitive experiments will be designed to examine the contribution of the open-ocean and local forcing through removing the KC and wind stress separately. Furthermore, the Luzon Strait, Taiwan Strait and Tsushima Strait will be closed one by one to study the mechanism of circulations in the ECYS, and the referred names and configuration of these experiments are shown in Table 1.

[9] The paper is organized as follows. The model, its setup and its forcing fields will be introduced in section 2. The results will be presented and discussed in section 3, which will be followed by a summary of this paper.

2. The Model and Forcing Fields

[10] The model is the latest version of POM model. It includes thermodynamics and the level-2.5 Mellor-Yamada

Table 1. Comparison of the *Control Run* and Sensitive Experiments

Experiments	Configuration
Control run	Full forcing
Sen-exp1	Removing the local wind stress
Sen-exp2	Blocking the Luzon Strait
Sen-exp3	Removing the KC
Sen-exp4	Blocking the Taiwan Strait
Sen-exp5	Blocking the Tsushima Strait

turbulence closure [*Mellor and Yamada*, 1982]. The model domain (100°–150°E, 0°–50°N) and topography are shown in Figure 1. The model resolution is 1/6° by 1/6° horizontally and 16 sigma levels vertically with a finer resolution for the upper layers. The bathymetry used in the model is interpolated from ETOPO5 5 min gridded elevation data [*NOAA*, 1988]; the minimum and maximum depth is set to 10 m and 3000 m, respectively.

[11] The model is initialized with temperature and salinity fields for January from the World Ocean Atlas 2001 (WOA01) [*Stephens et al.*, 2002; *Boyer et al.*, 2002], and is forced by monthly mean climatologic atmospheric fields. The wind stress and buoyancy fluxes are from the International Comprehensive Ocean-Atmosphere Data Set (ICOADS) [*Worley et al.*, 2005]. The buoyancy flux used in the model is net heat flux forcing, which is sensitivity to Sea Surface Temperature. Figure 2 shows the wind stress (arrow) and net heat flux (contour) at the surface of the ECS both in winter and summer. From Figure 2 we can find that the wind stress is northward and the ocean releases heat in winter and on the contrary in summer. Note that the horizontal gradient of net heat flux in winter is much larger than that in summer. The maximum of net heat flux is in the region of the KC in winter, while is in the coastal region in summer. Along the northern, southern, western and eastern boundaries, we specify model variables (T, S and velocity) from the results of a global model run [*Qiao et al.*, 2004].

[12] *Qiao et al.*'s [2004] model domain is from 75°S to 65°N, and the horizontal resolution is 1/2° by 1/2°. The east and west boundaries are set as continuous conditions, while the north and the south boundaries are set as solid conditions in the global model. *Qiao et al.*'s [2004] model together with their other results [*Xia et al.*, 2004] simulates the coastal circulation well and can provide open boundary conditions for fine resolution regional ocean circulation models. To the east of 130°E near the south boundary of our model, there is a small anticyclonic circulation, which is considered as the New Guinea Coastal Current and Halmahera Eddy. The former flows northward throughout the year, while the latter changes its sense of rotation during a few months, what is consistent with *Tomczak and Godfrey* [1994]. To the east of Philippines, seasonal variations are evidenced in transport of the KC as well as the bifurcation point of the North Equatorial Current [*Qiu and Lukas*, 1996; *Qu et al.*, 1998]. The bifurcation point moves northward in winter and southward in summer [*Qiu and Lukas*, 1996; *Qu and Lukas*, 2003], accomplished by a quantitative change in the partition of the North Equatorial Current transport between the KC and the Mindanao Current. Thus, the Kuroshio transport east of Luzon reaches its seasonal minimum in winter and seasonal maximum in summer. All of those can be found clearly in the model results.

[13] The SCS is a semienclosed marginal sea that connects with the Pacific Ocean through the deep Luzon Strait, with the ECS through the shallow Taiwan Strait, and with the Java and Sulu seas through the shallow Karimata and Mindoro Straits. The model shows that there is a big cyclonic circulation that occupies the whole basin of the SCS in winter. In summer, there is an anticyclonic circulation in the

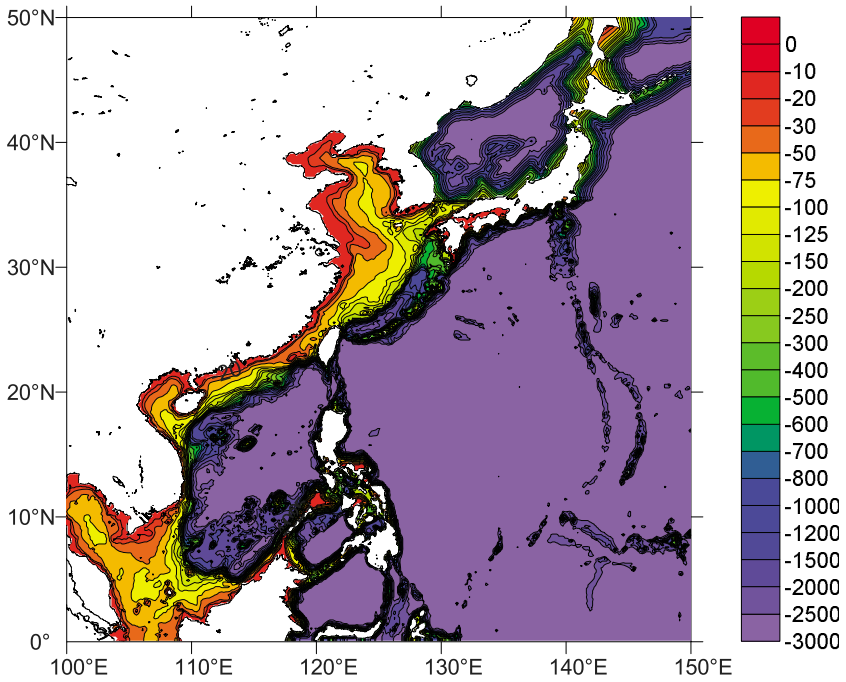

Figure 1. Model domain and topography (m). The minimum and maximum depths are set as 10 m and 3000 m, respectively.

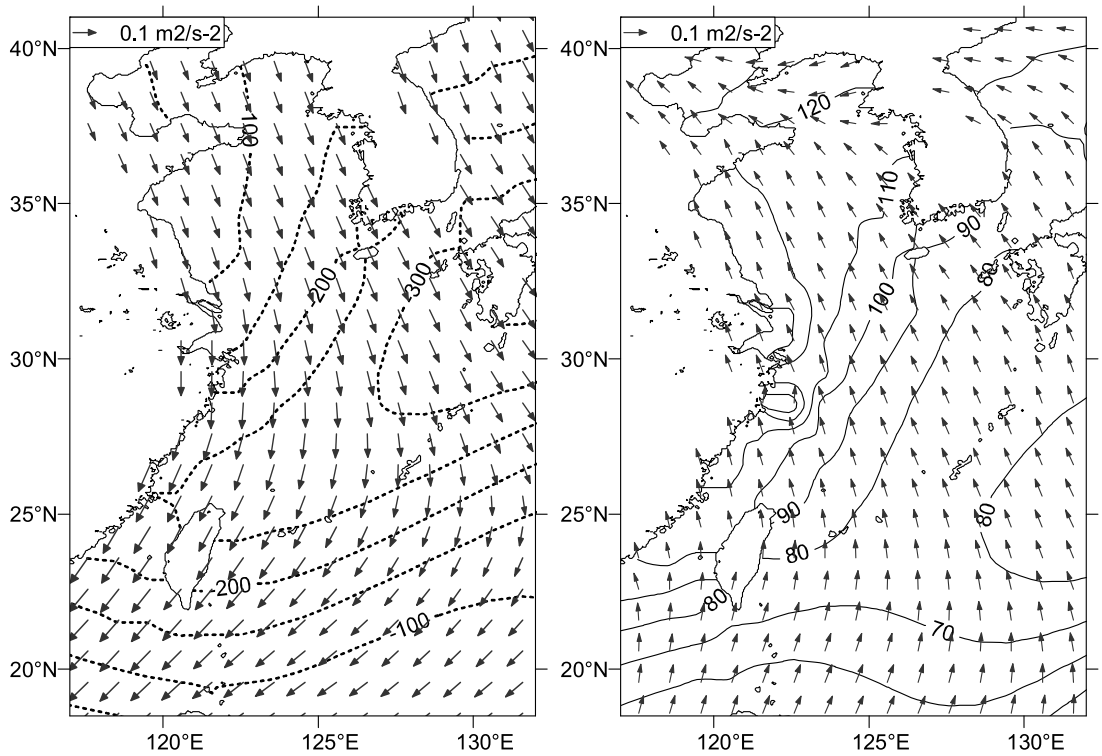

Figure 2. Net heat flux (contours, W m^{-2}) and wind stress (arrows, m^2 s^{-2}) at surface of the ECYS in (left) winter (averaged over February in the last model-run year) and (right) summer (averaged over August in the last model-run year). Here, the negative net heat flux means an oceanic heat loss, and the positive heat flux denotes an oceanic heat gain. The contour interval is 50 W m^{-2} in winter and 10 W m^{-2} in summer, respectively.

southern part and a cyclonic circulation in the northern part of the basin. The pattern of the SCS circulation is similar to some previous results [e.g., *Fang et al.*, 1998]. An important aspect of the SCS circulation is the existence of a mean current through the SCS, consisting of inflow from the Kuroshio through the Luzon Strait and outflow primarily through the Taiwan, Karimata, and Mindoro Straits. This circulation has been called the South China Sea Throughflow [e.g., *Qu et al.*, 2005; *Wang et al.*, 2006; *Yu et al.*, 2007], and the schematic diagram of it was given by *Qu et al.* [2005, 2006, 2009].

[14] The total transport through the Luzon Strait is essentially westward, with a maximum in winter and a minimum in summer [*Qu*, 2000; *Chu and Li*, 2000; *Fang et al.* 2005; *Yaremchuk and Qu*, 2004], which is also in accordance with the model results. Unlike with the schematic diagram by *Qu et al.* [2006, 2009], there are many researches [e.g., *Su and Wang*, 1987; *Li et al.*, 1992, 1993; *Chen and Sheu*, 2006; *Chen et al.*, 2010] pointed out that the TSC is not directly from the Kuroshio intrusion in the Luzon Strait. For the south boundary of our model in the southern SCS, there is a seasonal cycle with the Karimata Strait transport, which is southward in winter and northward in summer, the range is from −2.5 Sv to 1.8 Sv, which is correspond with the previous studies. The annual mean outflow is about −0.2 Sv, which is low in comparison to some estimates [e.g., *Fang et al.*, 2005], but is similar to other results [e.g., *Yaremchuk et al.*, 2009]. For the south boundary in the southern Sulawesi Sea, there is a persistent southward flow through the Makassar Strait, with seasonal variability of larger transport in summer than in winter, and annual mean transport of about 9 Sv, which is comparable with *Susanto and Gordon* [2005]. The South China Sea Throughflow is believed to inhibit the Indonesian throughflow in the Makassar Strait [*Qu et al.*, 2005; *Tozuka et al.*, 2007, 2009]. The Mindoro Strait provides the only passage from the SCS deeper than 100 m, and half of the SCS throughflow exits the basin in the Mindoro Strait [*Yaremchuk et al.*, 2009]. Opening the Mindoro Strait causes the North Equatorial Current split point to move southward and increases the transport of the Kuroshio east of Luzon while decreasing the Mindanao Current. But opening or closing the Karimata Strait or the Mindoro Strait does not affect the transport of the Pacific to Indian Ocean throughflow [*Metzger and Hurlburt*, 1996]. Thus, the south boundary of the SCS, which is referred to Karimata Strait transport in the model, may not the determinant factor of the TSC, even for the no-Luzon Strait experiment.

3. Results and Analysis

3.1. Model Results From the Control Run

[15] In this section, the results from the standard model run (hereafter referred to as the *control run*) will be discussed and compared with observations. In the *control run* the model was integrated for 10 years until it reached a statistically steady seasonal cycle. The spin-up time scale for a baroclinic ocean with a size of the Pacific is much

longer than 10 years especially in higher latitudes within the model domain. The relatively short spin-up time in our model integration is due to the use of a small model domain that extends from 100°E to 150°E, shown in Figure 1. The boundary condition prescribed along 150°E from a coarse-resolution global model already contains the spin-up information in the vast interior to the east of 150°E.

[16] After the 10 years of spin-up, circulations are well established over the open ocean and in the adjacent seas. Figure 3 shows the vertically averaged velocity in the ECS in February (left, chosen to represent winter) and August (right, representing summer), respectively. The overall pattern of the circulation is remarkably similar to what was summarized in review papers by *Su* [2001], *Ichikawa and Beardsley* [2002], and *Isobe* [2008]. The most noticeable feature is a robust KC that flows northward starting from the coast of Philippines. The KC leaps across the Luzon Strait, flows along the east coast of Taiwan Island, continues northeastward along the continental slope in the ECS, and turns eastward to the south of Japan. There are some branches and regional recirculations on both sides of the KC. To the south of Japan, one branch intrudes shoreward and feeds the TsWC through the Tsushima Strait. In the shallow coastal seas, the Yellow Sea Warm Current (YSWC) penetrates northward along the Yellow Sea Trough, and brings the warm and saline water toward the Bohai Sea.

3.1.1. Taiwan Strait Current

[17] The vertical distribution of the meridional velocity across 24.5°N at the Taiwan Strait is shown in Figure 4 for both winter (Figure 4, top) and summer (Figure 4, bottom). The maximum velocity occurs right along the west coast of Taiwan Island in either season. This is consistent with *Yang*'s [2007] hypothesis that a large KC-induced Δp between the northern and the southern tip of Taiwan Island would force a strong boundary current on the eastern side of the strait. Overall, the northward velocity is much stronger in the summer than in the winter. In fact, a narrow southward flow, associated with the winter China Coastal Current, is present at the western end of the strait. This current is forced by the local wind stress as we will discuss further when the results from sensitivity experiments are introduced. It is interesting to note that there is a local velocity maximum in the middle of the strait in the winter (Figure 4, top). The velocity field shown in Figure 3 seems to indicate that the flow through the central strait continues northward and later connects to the YSWC.

[18] The seasonal variations of the volume transport of the TSC in the *control run*, and all sensitivity experiments are shown in Figure 5 (the positive value means flows northward). In the *control run*, the TSC flows northward perennially and varies seasonally from the minimum of 1.5 Sv in the late fall to the maximum of 2.75 Sv in summer. *Fang et al.* [1991] used observations to estimate that the TSC varies from 1 Sv in fall to 3.1 Sv in summer. For the annually averaged transport, the model is close to 2 Sv reported by *Fang et al.* [1991]. However, the magnitude of the seasonal variability is considerably smaller. The minimum transport is also much larger than the 0.14 Sv observed by *Teague et al.* [2003] for the period from October to December 1999. *Isobe* [2008] estimated direct current measurements from various research projects, and calculated the throughflow transport in the Taiwan Strait is about 1.3 Sv, with a deviation from 0.1 Sv to 2.5 Sv. It is not clear why there is such a large discrepancy for the seasonally minimum transport. Interannual variability may have contributed to the difference.

3.1.2. Tsushima Strait Warm Current

[19] Another very interesting feature is the water mass sources that feed the TsWC into the Japan/East Sea (JES). There have been two traditional views regarding the source water of TsWC. It had been long considered that TsWC is fed by the Kuroshio branch current west of Kyushu [e.g., *Nitani*, 1972; *Lie and Cho*, 1994; *Lie et al.*, 1998]. This was challenged by *Beardsley et al.* [1985], who found that TsWC originated mainly from the Kuroshio branch current north of Taiwan. *Fang et al.* [1991] also found that the flow in the ECS, observed by current meters, was continuous between the Taiwan and Tsushima Straits. Meanwhile, *Lim* [1971] and *Sawara and Hanzawa* [1979] found that the water property in the Tsushima Strait was considerably different than that of KC, indicating that KC water was modified in the ECS before approaching the Tsushima Strait. *Isobe* [1999] reconciled these differences by proposing that the source water for TsWC may change seasonally. In the summer, the Kuroshio branch current north of Taiwan supplies the TsWC inflow to the JES in the summer season, while the Kuroshio branch current west of Kyushu takes over the supplier role in the winter.

[20] Although the dynamic processes that govern this seasonal alternation are not well understood, Figure 3, which shows the velocity field in both winter (Figure 3, left) and summer (Figure 3, right), appears to catch this seasonal alternation. The bold arrows are added on top of the model generated velocity vectors to highlight the large-scale flow directions. A careful examination of the velocity vectors in the upstream of TsWC shows that there is considerable seasonal variability. The TsWC source water derives from both the TSC and KC in either winter or summer. It also seems to have a seasonal preference. In winter the northward flow through the Taiwan Strait is weaker and confined to the eastern side along Taiwan Island's coast. The coastal current along the Chinese mainland is actually southward, consistent with observations. The northward TSC turns gradually offshore toward the shelf break where it meets the KC. It joins the KC branch current west of Kyushu and feeds the TsWC, an inflow into the JES. A large portion of the TSC-originated water has already joined the KC before reaching the Tsushima Strait, so it appears that the KC branch current west of Kyushu is the main source for the TsWC. In summer, the TSC is very robust and the flow is directed northward across the Taiwan Strait. The most noticeable difference from the winter pattern is that the flow over the broad ECYS is northward, especially off the coast of the Chinese mainland. Some of these northward shelf currents extend all the way up to the southern entrance of the Tsushima Strait. The KC branch current west of Kyushu is still robust and feeds the TsWC. But it is no longer the only dominant source in summer. The TsWC source water derives from both the KC and the flow through Taiwan Strait in summer. The variation of TSC transport through the Taiwan Strait and the change of the shelf current pathways over the ECYS are two main factors that affect the seasonal preference of the TsWC source waters. The seasonal origin of the TsWC is strongly depended on the mixing scheme of the

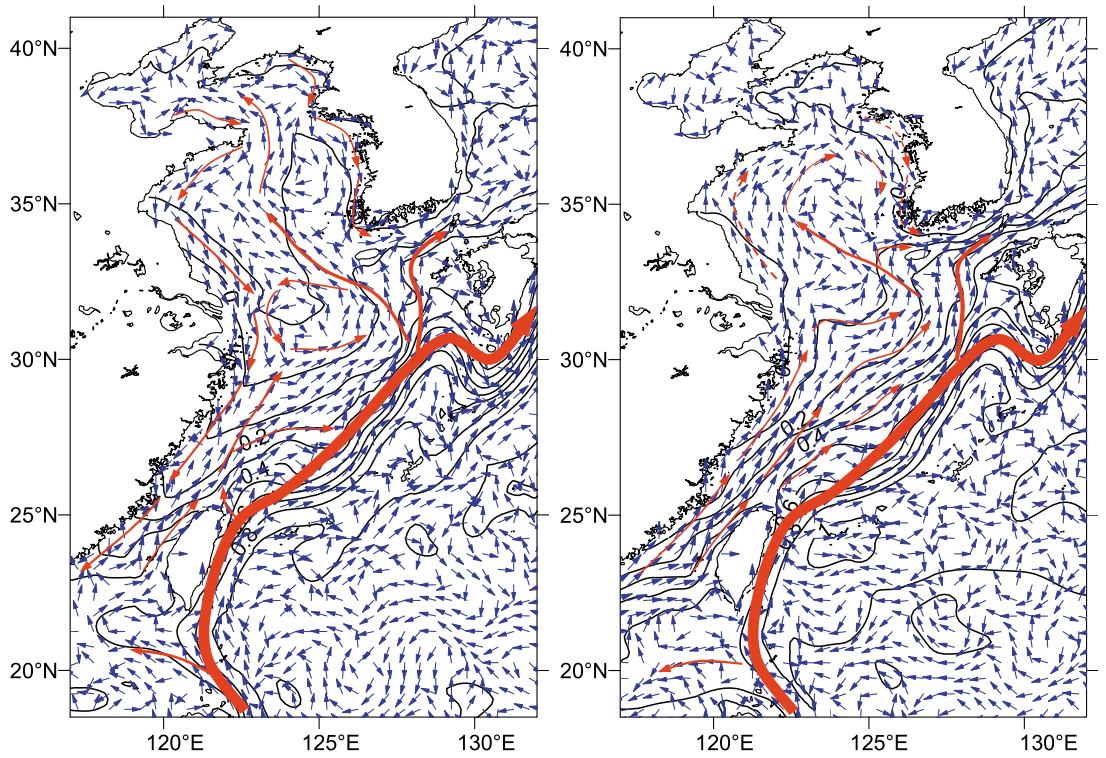

Figure 3. Sea surface height (contours, m) and depth-averaged velocities (arrows, m s^{-1}) of the ECYS in (left) winter (averaged over February in the last model-run year) and (right) summer (averaged over August in the last model-run year) from *control run*. The contour interval is 0.1 m. The bold arrows added on top highlight the large-scale flow directions.

model. Actually, many studies [e.g., *Lie and Cho*, 1994; *Isobe*, 1999, 2000] have been done attributing it to the thermohaline or density field, which is essentially the mixing effect among some of the KC branch water, ECS water, Changjiang diluted water, and so on. In another work by *Guo et al.* [2006], they found that the baroclinic effect also plays an important role in the KC onshore intrusion and origin of the TsWC.

[21] The meridional velocity section across the Tsushima Strait is shown in Figure 6 for both summer and winter seasons. Results from a very comprehensive survey of the velocity filed has been published recently [*Takikawa et al.*, 2005] and thus are used to compare with the model results here. *Takikawa et al.* [2005] calculated the transport by using the data collected long-term ADCP on a ferryboat between Hakata and Pushan. The 5 year averaged transport since February 1997 was 2.64 Sv with 1.1 and 1.54 Sv in the eastern and western channels, respectively. The transport in either the eastern or western channel varies considerably with season. The 5 year averaged transport is minimum in January and maximum in October. In the same work as mentioned above, *Isobe* [2008] estimated the throughflow transport in the Tsushima Strait on the basis of some previous research, and obtained the average result of about 2.6 Sv, with a variation from 1.2 Sv to 4 Sv. The model compares quite well with the observation (the monthly velocity profiles plotted in Figure 4 of *Takikawa et al.*'s [2005] paper). The patterns in both the eastern and western channels are remarkably similar. The model also simulates successfully the reversed flow on two side edges in the eastern channel, a prominent feature revealed by *Takikawa et al.*'s [2005] analyses. The velocity magnitude is a bit weaker in the model than in the data, especially in the summer and along the western channel. This is, at least partially, due to the fact that velocity plotted in Figure 6 is the meridional velocity, while *Takikawa et al.* [2005] used the along-channel velocity. Both channels are oriented in the northeastern direction and thus the along-channel flow has both northward and eastward velocity components. The total velocity is greater than the meridional component alone. The annually mean transport in the model, a bit over 3 Sv combined both channels, is actually greater than the 2.64 Sv reported by *Takikawa et al.* [2005], 2.7 Sv by *Teague et al.* [2002], and 2.6 Sv by *Isobe* [2008].

3.1.3. Yellow Sea Warm Current

[22] It is interesting to note that the YSWC becomes much less intrusive in summer and is limited mostly in the southern trough, contrasting with a deep winter penetration well into the trough. This seasonal characteristic agrees well with observations [*Park*, 1986; *Lie*, 1986]. The observational evidence of YSWC's existence is mostly circumstantial and often derived from the water mass characteristics. The less intrusive nature of the YSWC has prompted a debate regarding whether the YSWC should be regarded as a persistent mean current [e.g., *Lie et al.*, 2001]. To the east of the YSWC, there is a perennial southward flow along the west coast of Korea. This current was referred to the Korea Coastal Current in some previous studies. *Yang* [2006] argued that the Korea Coastal Current is induced by the TsWC as a source- and sink-driven flow along bathymetry, which itself is forced by the KC through the pressure gap between the Tsushima and Tsugaru Straits.

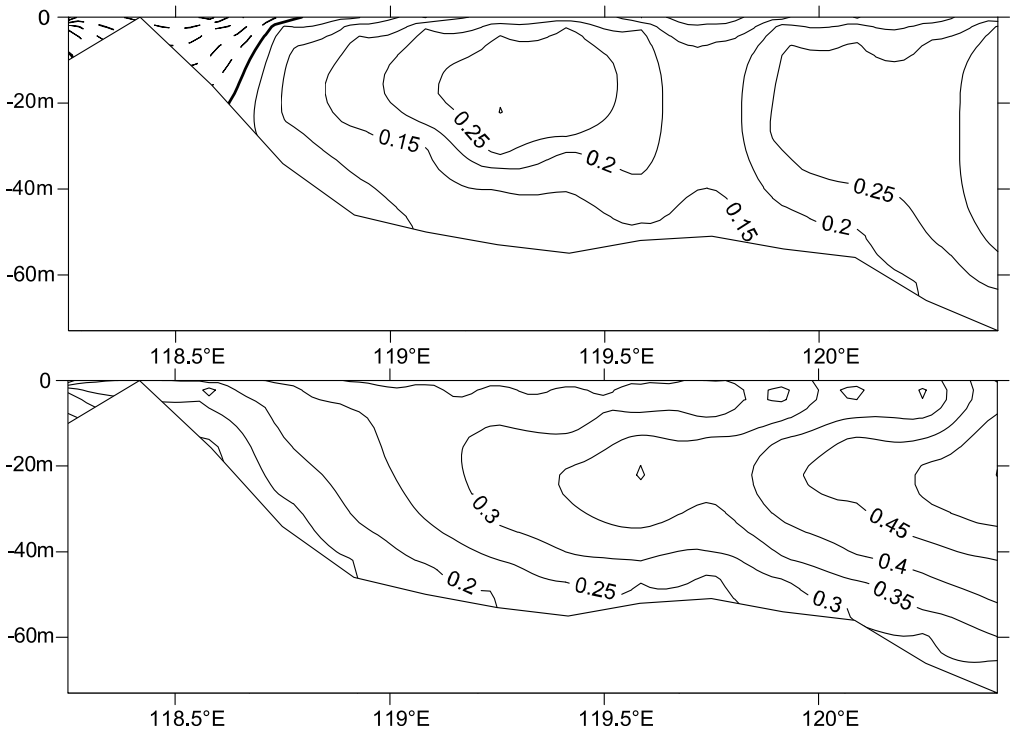

Figure 4. The vertical sections of meridional velocity (m s^{-1}) across 24.5°N at the Taiwan Strait in (top) winter (averaged over February in the last model-run year) and (bottom) summer (averaged over August in the last model-run year). The positive velocity means northward flow, and the negative velocity denotes southward flow. The contour interval is 0.05 m s^{-1}. Note that the northward velocity is much weaker in the winter. A southward China Coastal Current is evident along the western side of the strait.

[23] Figure 7 shows the meridional velocity across 35°N at the Yellow Sea. From Figure 7 we can find that, the flow in the surface is southward in winter (Figure 7, top), especially two strong coastal currents along both China and Korea sides. In the lower layer, there is northward flow along the Yellow Sea Trough, which is called the YSWC. In summer (Figure 7, bottom), the flow in the surface is northward, except that there is a southward flow near the Korean coast, which itself may be induced by the TsWC. In the lower layer, the flow is very week, but there still exists a northward flow along the western Yellow Sea Trough.

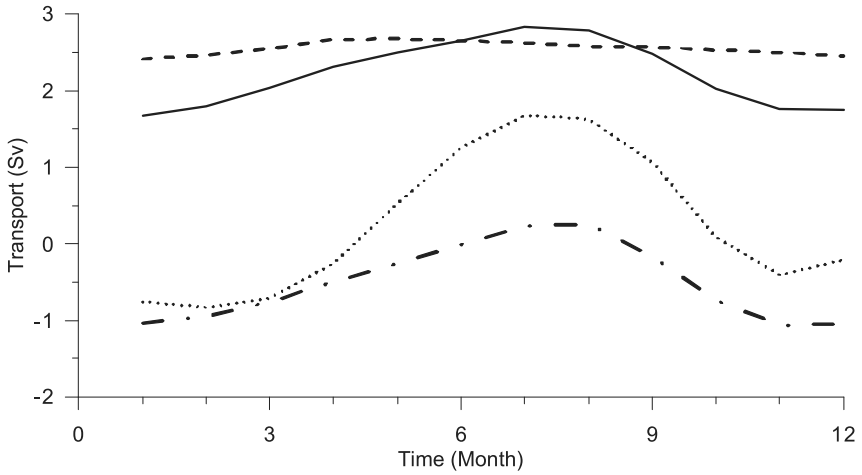

Figure 5. The monthly averaged volume transport (Sv) of the TSC from *control run* (solid line), *sen-exp1* (dashed line), *sen-exp2* (dotted line), and *sen-exp3* (dash-dotted line). The positive transport means northward flow, and the negative transport denotes southward flow.

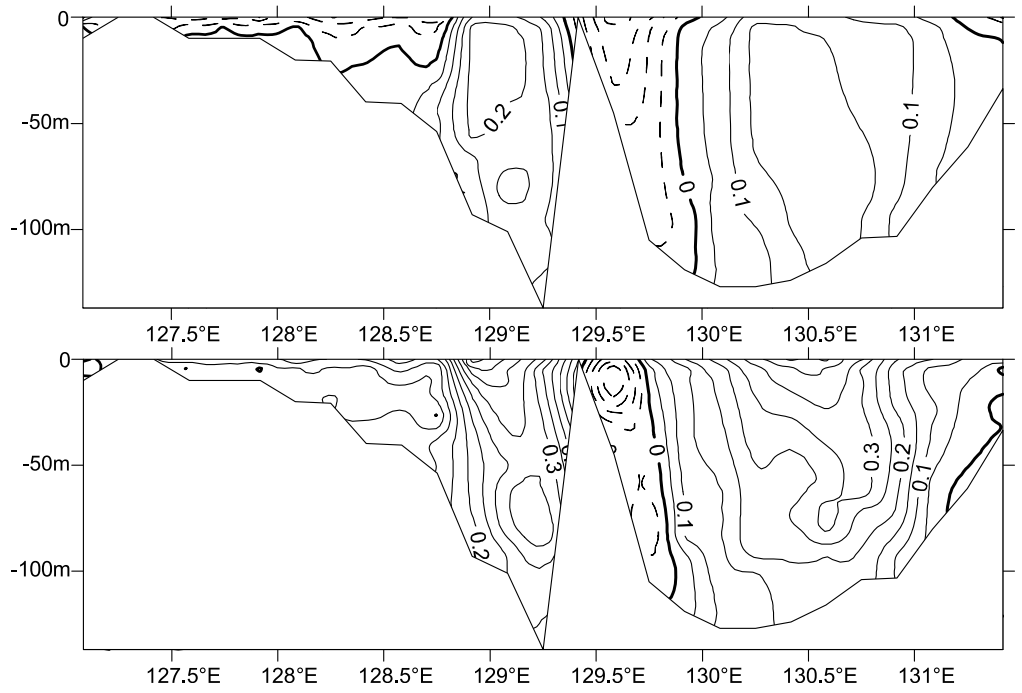

Figure 6. The vertical sections of meridional velocity (m s^{-1}) across 34.5°N at the Tsushima Strait in (top) winter (averaged over February in the last model-run year) and (right) summer (averaged over August in the last model-run year). The positive velocity means northward flow, and the negative velocity denotes southward flow. The contour interval is 0.05 m s^{-1}.

[24] The time series of velocity fields and sea surface heights anomaly of the Yellow Sea in winter are given in Figure 8. The time series are 1 h, 7 h, 13 h, 19 h, 25 h, 37 h, 49 h, and 73 h since from the winter monsoon is set up. Here we try to give the adjustment processes of the YSWC for the purpose of starting further research. When the winter monsoon is prevalent, the southward wind will induce a downwind flow in the whole Yellow Sea (Figure 8a), and

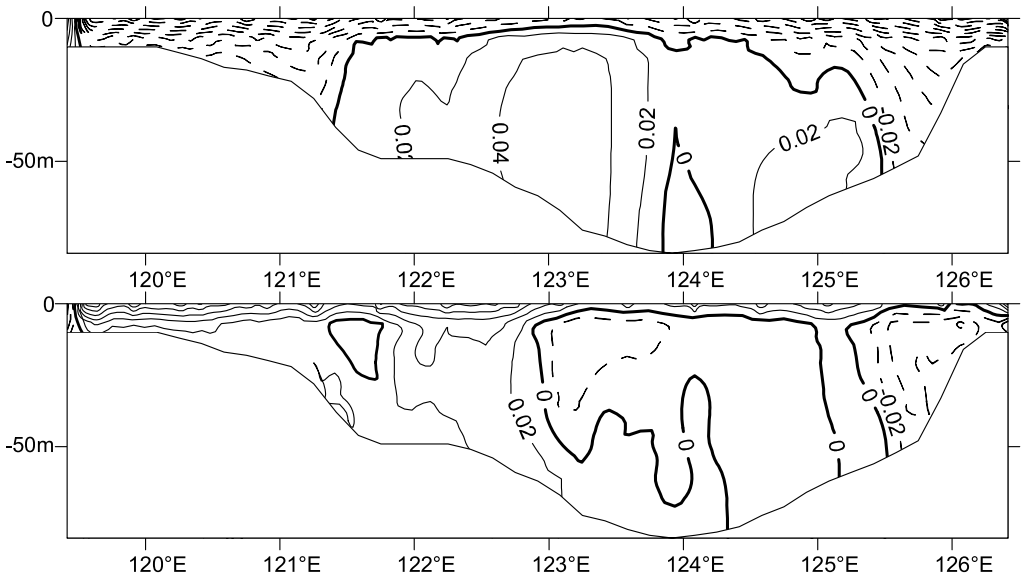

Figure 7. The vertical sections of meridional velocity (m s^{-1}) across 35°N at the Yellow Sea in (top) winter (averaged over February in the last model-run year) and (bottom) summer (averaged over August in the last model-run year). The positive velocity means northward flow, and the negative velocity denotes southward flow. The contour interval is 0.02 m s^{-1}.

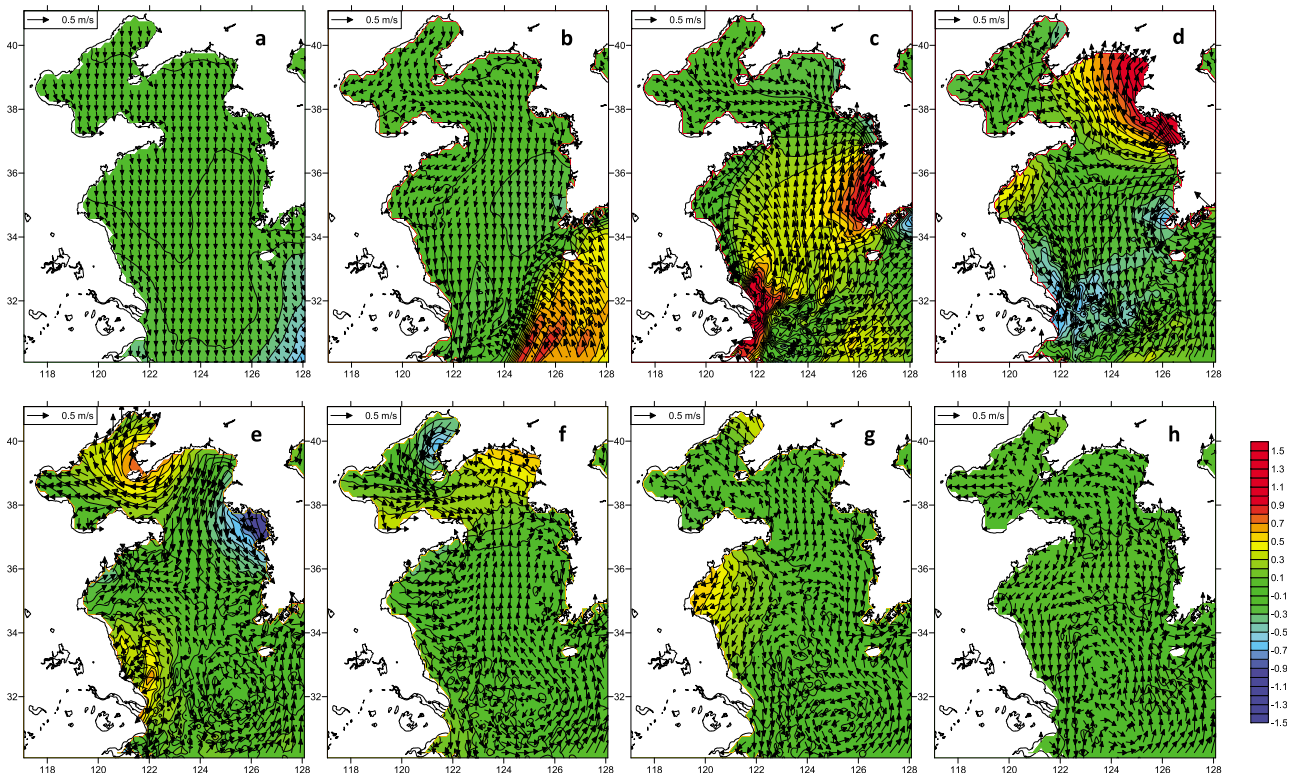

Figure 8. The time series of sea surface heights anomaly (contours, m) and depth-averaged velocity fields (arrows, m s^{-1}) of the Yellow Sea in winter. The time series are (a) 1 h, (b) 7 h, (c) 13 h, (d) 19 h, (e) 25 h, (f) 37 h, (g) 49 h, and (h) 73 h, from since the winter monsoon was set up. The contour interval is 0.1 m.

will cause a northward sea level slope first. According to the wave dynamics, there will be westward propagating long Rossby waves from the eastern boundary. As the Rossby radius of deformation changes meridionally, the waves will propagate faster in the southern part than in the northern part, which will result in a northwestward sea level slope (Figure 8b). The flows along the Chinese and Korean coasts still head southward, but the circulation in the Yellow Sea Trough turns in a clockwise direction. Then there should be a northward flow to compensate the southward flows along the west and east coasts of the Yellow Sea (Figure 8c). Meanwhile, the southward wind stress forms the coastal upwelling along the southwestern coast of Korea Peninsula, this upwelling enhances the Korea Coastal Current in winter, this feature propagates counterclockwise around the Yellow Sea and Bohai Sea's trough not only as the coastal Kelvin wave but also as the topographic Rossby wave (Figures 8d–8g). As time goes on, the sea level of the central Yellow Sea will be higher in the eastern part than in the western part, which forms a high sea level tongue in the eastern part and a low sea level tongue in the western part. Near the front, there is a northward flow which is widely considered the YSWC (Figure 8h). Moreover, the topographic Rossby waves/boundary Kelvin waves may continuous propagate southward along the Chinese coast to the Taiwan Strait, and affect the sea level and current in the strait.

3.1.4. Momentum Balance Around Taiwan Island

[25] The depth-integrated momentum fluxes along the coast of Taiwan Island are calculated by source code of the standard model. The momentum equations in sigma-coordinate are derived from POM model, that is

$$\begin{aligned}
&\frac{\partial UD}{\partial t}\frac{\partial U^2 D}{\partial x}+\frac{\partial UVD}{\partial y}+\frac{\partial U\omega}{\partial \sigma}-fVD+gD\frac{\partial \eta}{\partial x}\\
&\quad+\frac{gD^2}{\rho_0}\int_\sigma^0\left[\frac{\partial \rho'}{\partial x}-\frac{\sigma'}{D}\frac{\partial D}{\partial x}\frac{\partial \rho'}{\partial \sigma'}\right]d\sigma'=\frac{\partial}{\partial \sigma}\left[\frac{K_M}{D}\frac{\partial U}{\partial \sigma}\right]\\
&\quad+\frac{\partial}{\partial x}\left[2DA_M\frac{\partial U}{\partial x}\right]+\frac{\partial}{\partial y}\left[DA_M\left(\frac{\partial U}{\partial y}+\frac{\partial V}{\partial x}\right)\right],\\
&\frac{\partial VD}{\partial t}+\frac{\partial UVD}{\partial x}+\frac{\partial V^2 D}{\partial y}+\frac{\partial V\omega}{\partial \sigma}+fUD+gD\frac{\partial \eta}{\partial y}\\
&\quad+\frac{gD^2}{\rho_0}\int_\sigma^0\left[\frac{\partial \rho'}{\partial y}-\frac{\sigma'}{D}\frac{\partial D}{\partial y}\frac{\partial \rho'}{\partial \sigma'}\right]d\sigma'=\frac{\partial}{\partial \sigma}\left[\frac{K_M}{D}\frac{\partial V}{\partial \sigma}\right]\\
&\quad+\frac{\partial}{\partial x}\left[DA_M\left(\frac{\partial U}{\partial y}+\frac{\partial V}{\partial x}\right)\right]+\frac{\partial}{\partial y}\left[2DA_M\frac{\partial V}{\partial y}\right],
\end{aligned}\tag{1}$$

where (x, y, z) are the Cartesian coordinates; $D = H + \eta$ where H is the bottom topography and η is the sea surface elevation; $\sigma = (z - \eta)/(H + \eta)$ thus σ ranges from $\sigma = 0$ at $z = \eta$ to $\sigma = -1$ at $z = -H$; ρ_0 is the reference density; $\rho' = \rho - \rho_{MEAN}$ where ρ is the in situ density and ρ_{MEAN} is horizontally averaged, time-independent initial density field; U and V are the depth-dependent horizontal velocity components; and ω is the transformed vertical velocity. Other variables are the Coriolis parameter f, gravitational acceleration g, horizontal viscosity coefficient A_M, and vertical viscosity coefficient K_M.

[26] The momentum balance consists of terms for acceleration (Inertia term: first term on the left), advection in the horizontal and vertical directions (second to fourth term on the left), Coriolis force (fifth term on the left, vanishes in the momentum balance along the boundary owing to the no-normal flow condition), baroclinic term (sixth term on the left), pressure gradient (first term on the right), vertical diffusion (second term on the right, including negative Wind stress and Bottom friction), and horizontal diffusion (third and fourth term on the right), in that order. The differences from the barotropic model by *Yang* [2007] are that it involves the baroclinic effect, and the bottom friction of Rayleigh relation is replaced by a quadratic drag relation. The *i*th momentum flux is integrated clockwise along the coast of Taiwan Island as the following form: $M_i = \int_0^s \vec{m}_i \cdot \vec{l}\, ds$, where $\vec{l}$ is unit vector tangential to the lateral boundary.

[27] As the integral of the momentum fluxes around the island is near zero, we didn't show it around the whole island, instead of integral along the west coast of the island. The one-side momentum balance can help to examine the importance of pressure gradient in dominating the flow direction. Figure 9 shows the monthly variability of the integrated primary terms in the momentum balance. The positive value means clockwise along the coast of Taiwan (note that the pressure gradient, wind stress, bottom stress and horizontal diffusion shown in Figure 9 are negative corresponding terms in the momentum equation, thus the sum of these terms will be balanced to that of other terms). The time rates of change in the momentum balance are calculated. The annual rates of change in inertia term, advection, baroclinic term, pressure gradient, wind stress, bottom friction and horizontal diffusion are about −0.4, −0.2, −3.0, −4.0, −0.1, 0.6 and 0.2 ($m^3\ s^{-2}\ month^{-1}$) in turn. The annual variation is very small but seasonal variation is relatively obvious, which may be dominated by the wind stress and baroclinic effect. The annual mean values of these terms are also given, which are about −1e-5, −0.004, 0.045, 0.145, −0.034, −0.065 and −0.005 ($10^3\ m^3\ s^{-2}$) in turn. We can find that the inertia term is so small that the flow can be considered as a steady state, and the pressure gradient is the dominant in the momentum fluxes. The bottom friction no doubt is against the flow, and the wind stress and baroclinic effect mainly contribute to its seasonal variability. It is the pressure gradient that plays a decisive role in setting the direction of flow through the strait. So the steady and barotropic model used by *Yang* [2006] appears to capture the essential dynamics that govern the annual mean flows over the ECYS. But for the seasonal variability, it is no doubt necessary to employ a baroclinic model.

3.2. Sensitivity Experiments

[28] The results from the *control run* are reasonably consistent with observations. This gives us a level of confidence to examine the mechanism by using this 3-D model. Here we revisit the mechanism that governs the flow through the Taiwan Strait. The Taiwan Island is located at the edge of shelf break. The KC flows along the east coast of the island and exerts a large friction along the boundary as can be explained in terms of the western boundary layer dynamics. The friction has to be balanced by a considerable pressure gradient from the southern to the northern tip of the island (the Coriolis term vanishes in the momentum balance along the boundary owing to the no-normal flow condition). This KC-induced pressure difference between the northern and southern tip of the island is felt identically along the island's west coast in the Taiwan Strait, and forces a northward flow parallel to the KC. The local wind stress tends to weaken but is insufficient to suppress the TSC. A follow-up study by J. Yang et al. (Open-ocean forcing of a semi-enclosed marginal sea: Topographic effect on the Tsushima Warm Current, submitted to *Journal of Physical Oceanography*, 2010) showed that the TsWC makes an important secondary contribution to the northward transport across the Taiwan Strait. The connection between flows on two sides of the island can be demonstrated eloquently by a classic theorem in fluid dynamics. By following *Pedlosky et al.* [1997], one can integrate a momentum equation of a one-layer fluid (either a barotropic model layer or a layer of water in a 3-D model). The integration of the nonlinear momentum advection terms vanishes. The Coriolis term is zero for the momentum balance in the along-boundary direction owing to the no-normal flow contention. The pressure is continuous around the island so that the integral of its gradient is zero. The integral balance yields

$$\frac{\partial}{\partial t}\left(\oint_C \vec{u}\cdot d\vec{l}\right) - \oint_C (\vec{\tau}_S - \vec{\tau}_B)\cdot d\vec{l} = 0. \tag{2}$$

Here, $\vec{\tau}_S$ is the surface wind stress, $\vec{\tau}_B$ is the bottom drag, C is the integration contour around the island, and $d\vec{l}$ is the unit tangent vector to the island. For an unforced and inviscid fluid, the second term vanishes, and so equation (2) becomes the classic Kelvin theorem of the conservation of circulation around an island. *Yang* [2007] used the steady assumption and thus the integrals of friction and wind stress balance each other, that is,

$$\oint_C (\vec{\tau}_S - \vec{\tau}_B)\cdot d\vec{l} = 0. \tag{3}$$

[29] If the local wind stress is weak or equivalent along both sides of the island, the integral of the friction must then be zero. In the TSC application, *Yang* [2007] argued that the mighty KC flows northward at the east of Taiwan Island and results in a strong anticyclonic drag. If the wind stress is not strong enough to overcome the bottom stress, then a northward current must exist there, and it is the reason why the TSC flows northward all through the year.

[30] In order to test this mechanism in a time-dependent and 3-D model, several experiments are designed here: (1) removing the local wind stress (*sen-exp1*), (2) blocking the Luzon Strait (*sen-exp2*), and (3) removing the KC (*sen-exp3*). All the sensitivity experiments start from rest state with January temperature and salinity of WOA01, and are integrated for 10 years as well as the control run. The referred names and configuration of these experiments are shown in Table 1. The results will be compared with the *control run* shown in Figure 3.

3.2.1. Sen-exp1

[31] In the first sensitivity experiment (*sen-exp1*), the wind stress is removed from the model domain shown in Figure 1. The only forcing is through the prescribed lateral boundary conditions. The model starts from zero, and is integrated 10 years as the control run. This experiment is

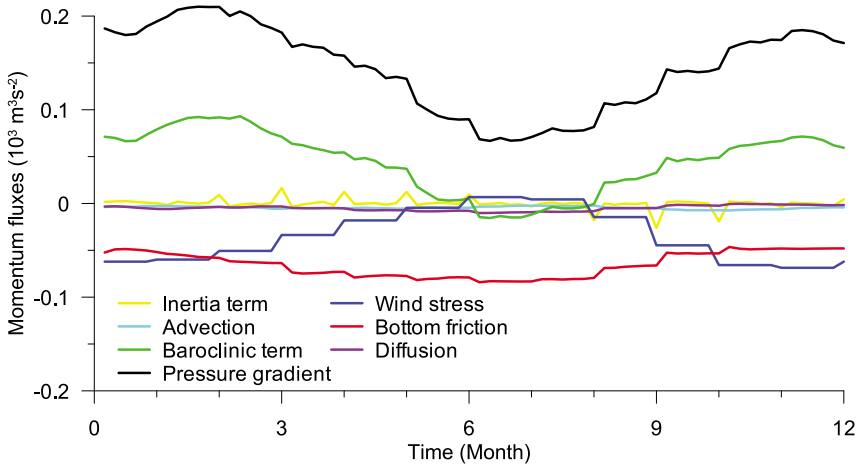

Figure 9. Primary terms (m^3 s^{-2}) in the momentum balance integrated along the west coast of Taiwan Island. The positive value means clockwise around the coast of Taiwan Island.

equivalent to the KC Run discussed by *Yang* [2007] since the flow through the lateral boundaries contains the information of the Sverdrup dynamics in the vast interior ocean. Figure 10 shows the depth-averaged velocity field in winter (Figure 10, left) and summer (Figure 10, right), respectively. All major currents in the area, including the TSC, TsWC, YSWC and Korea Coastal Current, remain robust even though there is no direct wind stress forcing locally. This is consistent with the barotropic model results reported by *Yang* [2007], and thus supports their assertion that these currents are primarily induced by forcing over the open ocean. The circulation around the Taiwan Island is nearly steady, and so the integral balance in this model run without local wind stress is

$$\int_C \vec{\tau}_B \cdot d\vec{l} = 0. \tag{4}$$

The accumulated friction exerted by the KC along the east coast of Taiwan Island must be balanced by that along the

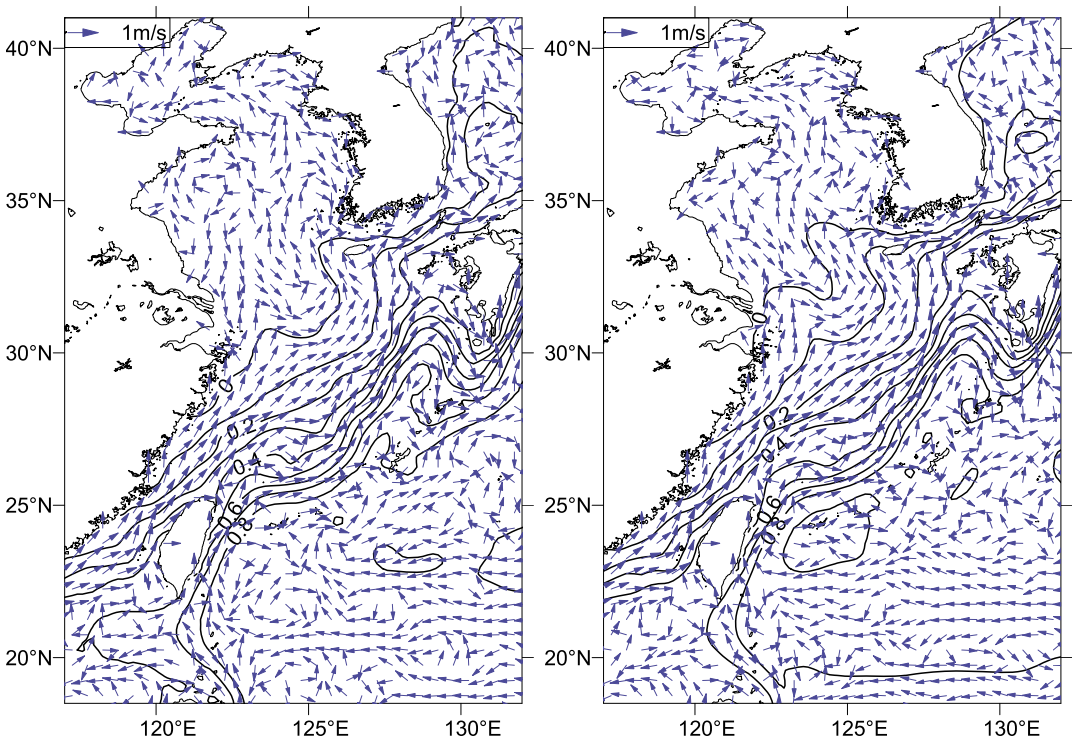

Figure 10. Sea surface height (contours, m) and depth-averaged velocities (arrows, m s^{-1}) of the ECYS in (left) winter (averaged over February in the last model-run year) and (right) summer (averaged over August in the last model-run year) from *sen-exp1*. The contour interval is 0.1 m.

west coast. This requirement results in a northward flow along the Taiwan Strait parallel to the KC. We integrate the friction around the Taiwan Island, and the outcome indeed satisfies the assumption.

[32] It is interesting to note that the circulation in the region exhibits little seasonal variability. The remarkable steadiness of all major currents contrasts strongly with large seasonal variations in the *control run* (Figure 3). Overall, the circulations from this experiment resembles more closely with the summer flow in the *control run* (Figure 3, right). This is perhaps due to the relative weakness of the monsoonal wind in the summer season. Without the local wind stress forcing, the flow through the Taiwan Strait is northward across the whole channel in both winter and summer (Figure 10). The southward flow along the Chinese mainland coast virtually disappears all the way from the Bohai Sea to the SCS. The YSWC shows little seasonal changes, consistent with *Mask and O'Brien* [1998], who suggested that the seasonal variability of YSWC may be due to the local monsoonal forcing. In the steady forcing case, the YSWC and the Korea Coastal Current are induced by the TsWC in the form of source- and sink-driven flow over the shelves in the ECYS. The winter strengthening of the YSWC shown in the *control run* (Figure 3) is unlikely due to the direct wind stress forcing since it flows against the prevailing northeasterly wind. It is probably related to the southward flow along the Chinese mainland and Korean coast (Figure 3, left). The winter wind forces a southward boundary current along the entire coast of the Chinese mainland, and strengthens the southward Korea Coastal Current simultaneously. Owing to the continuity requirement, water has to be drawn into the northern Yellow Sea and the Bohai Sea to feed the boundary current. Therefore, the water mass is sucked into the region through the Yellow Sea Trough, and thus results in a deep penetration of the YSWC in the winter season. We have mentioned before that the ocean receives heat flux in summer at the Yellow Sea, which will decrease density, increase buoyancy and make the stratification stability in surface. This may be a contributing factor in formation of the famous Yellow Sea Cold Water Mass, which itself may weaken the YSWC in summer. These issues could not be addressed in steady models like the one used by *Yang* [2007, 2006].

3.2.2. Sen-exp2

[33] In the second sensitivity experiment (*sen-exp2*), the Luzon Strait between Taiwan Island and Philippines is blocked. The forcing includes the local wind stress and exchanges through all lateral boundaries, just like in the *control run*. For a model domain from 17° to 50°N, Taiwan Island is not treated as an island, and thus the integral constraint (1) no longer applies here (in a larger model domain, the combination of Taiwan Island and Philippines would make a large island, and the constraint would apply). The flow through the Taiwan Strait reverses seasonally from being southward in winter (Figure 11, left) to northward in summer (Figure 11, right), and is the same direction as the local wind stress. We would like to point out here that the KC forcing cannot be removed completely in this run. About 1/3 of the annual mean transport through the Taiwan Strait is due to the remote forcing of TsWC. Like the Taiwan Island, the Kuroshio and Oyashio Currents along Japan's east coast will set the pressure gradient between the Tsushima and Tsugaru Straits. The pressure gradient can also be felt along the west coast of Japan, and induces a northward flow through the Tsushima Strait. Theoretically, according to Island Integral Constraint, the Kuroshio and Oyashio Currents along Japan's east coast will induce anticyclonic friction, which should be balanced by cyclonic friction to the west coast of Japan, thus there is a current flows northward through the Tsushima Strait and one of its branches continues to flow northward along the west coast of Japan. For the mass conservation and coastal wave theory (propagating along the right boundary at Northern Hemisphere), it is plausible to assume that the TsWC transport through the Tsushima Strait will influence the upstream conditions in the ECYS as source- and sink-driven effect. This appears to explain why the southward flow in winter (Figure 11, left) is still weaker than the northward flow in summer (Figure 11, right) even though the magnitude of wind stress is much greater in winter than in summer.

3.2.3. Sen-exp3

[34] In the third sensitivity experiment (*sen-exp3*), the initial fields and surface forcing fields prescribed in the region studied are the same as *control run*, while the model variables are no longer prescribed along lateral boundaries. Instead, an open boundary condition is used to allow information to propagate outward. The small domain is effectively disconnected from the interior Sverdrup flow in this model set up. The KC is indeed weak and not well organized as a unidirectional current (Figure 12). As the cross-shelf pressure is balanced by the Coriolis Effect of the flow, it will have a great reduction compared with that in control run. Using the model results, we calculated the Sea Level difference between Ishigaki in the Southern Ryukyu Islands and Keelung on northeast Taiwan ($SL_{Ishigaki} - SL_{Keelung}$). In *control run*, the sea level difference between them is about 0.56 m in summer and 0.52 m in winter. While the sea level difference is significantly reduced in *sen-exp3*, which is 0.08 m in summer and even changes its sign to −0.02 m in winter. The flow is southward in winter and northward in summer through the Taiwan Strait and over the broad ECYS. The flow between the ECS and the JES, that is, the TsWC, reverses its direction seasonally without the KC forcing. This supports the claim that the TsWC is forced by the KC. The YSWC disappears in summer. Combined with the results shown in previous experiments, we conclude here that the YSWC is primarily forced by the KC through the TsWC, and the local wind stress only modulates its seasonal variability. Without the KC, the flow along the Yellow Sea Trough is very weak and disorganized in summer (Figure 12, right). But owing to the compensation for the southward coastal current induced by wind stress, the YSWC still exists and flows northward in winter (Figure 12, left).

[35] In *sen-exp1*, the model domain shown in Figure 1 is forced by wind stress and buoyancy over the open ocean and the local wind stress forcing is turned off. The TSC transport varies little with seasons (Figure 5, dashed line), indicating the important role of the local forcing in modulating the seasonal cycle. In other words, the northward transport is forced by the open ocean through the KC, but the seasonal variability is caused by the local monsoonal forcing. It is interesting to note that the annual mean transport in *sen-exp1* is slightly larger than that in the *control run*. It means that removing the local forcing of wind stress would result in a greater TSC transport, which is easy to

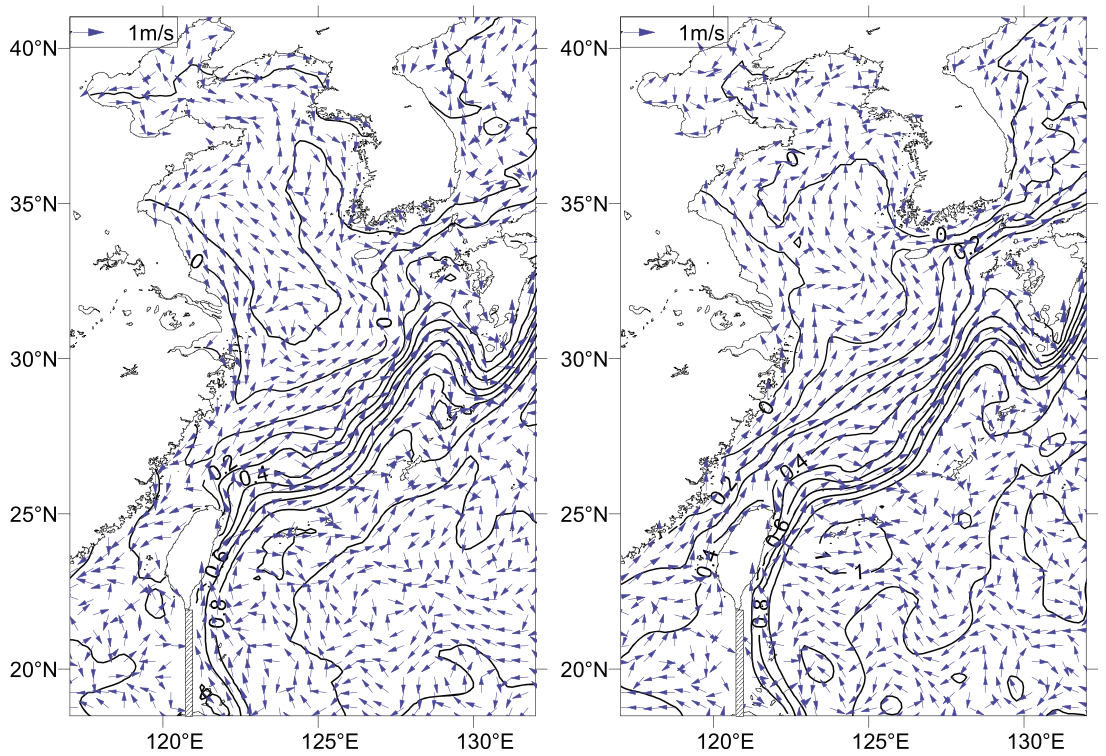

Figure 11. Sea surface height (contours, m) and depth-averaged velocities (arrows, m s^{-1}) of the ECYS in (left) winter (averaged over February in the last model-run year) and (right) summer (averaged over August in the last model-run year) from *sen-exp2*. The contour interval is 0.1 m.

understand. In the *control run*, the wind stress along the Taiwan Strait is southwestward in winter and northeastward in summer, but the annual mean is southwestward, which is against the flow direction and acts as an obstacle to the TSC. Consequentially, removing the restraint effect of wind stress will increase annual mean transport of the TSC. In *sen-exp2*, the Luzon Strait is blocked, and so the island integral constraint (2) voids. The TSC transport becomes much weaker as discussed earlier in this paper. The annual mean transport is still positive or northward (Figure 5, dotted line) owing to the remote forcing from TsWC. Without the KC forcing, in *sen-exp3*, the annual mean transport becomes even weaker (Figure 5, dash-dotted line).

[36] The integral constraint (2) is derived from using an assumption of steady state. The steady assumption remains valid for variability that has a time scale longer than what a coastal trapped wave would take to propagate around the Taiwan Island. For instance, a shallow-water gravity wave would take just days to complete the propagation around the island. So one would expect that constraint (2) remains a valid connecting mechanism for seasonal to interannual variability on flows on both sides of the island (this is supported by our preliminary results from multi-decadal runs).

3.2.4. Sen-exp4 and Sen-exp5

[37] To investigate the relationship between the Taiwan and Tsushima Straits, and their effects on circulations in the ECYS, two additional experiments are conducted here: blocking the Taiwan Strait (*sen-exp4*), and blocking the Tsushima Strait (*sen-exp5*). In the two experiments, the forcing is the same as *control run*, except that the two straits are blocked separately. From the results we can find that, when the Taiwan Strait is blocked (Figure 13), there will be no flow through the Taiwan Strait from the SCS to the ECS. But the circulation pattern of the ECYS almost remains the same as *control run*. While if the Tsushima Strait was blocked, the TsWC would disappear naturally. In winter, to compensate the wind-induced southward coastal currents along both China and Korea sides, the YSWC will flow northward as usual (Figure 14, left). But in summer, without the suction of the TsWC, the southward Korea Coastal Current will turn toward the wind direction, and the YSWC will also reverse as a compensation current (Figure 14, right).

[38] We also calculate the volume transport of the TsWC in *sen-exp4* (Figure 15) and that of the TSC in *sen-exp5* (Figure 16). We can find that the Tsushima Strait transport in *sen-exp4* has no evident change, while the Taiwan Strait transport in *sen-exp5* cuts its value by a third comparing with the *control run*. The two additional experiments can further validate source- and sink-driven flow by the Tsushima Strait, that is, on one hand, the TsWC will induce the southward Korea Coastal Current, and then breed the YSWC as a compensation flow; on the other hand, it will induce the flow along isobaths in the ECS, and contribution to the northward flow in the Taiwan Strait.

[39] Table 2 shows volume transports of the China Coastal Current, Yellow Sea Warm Current and Korea Coastal Current. It is easy to find from Table 2 that the YSWC transport is equivalent to the sum of the China Coastal Current transport and Korea Coastal Current transport, which

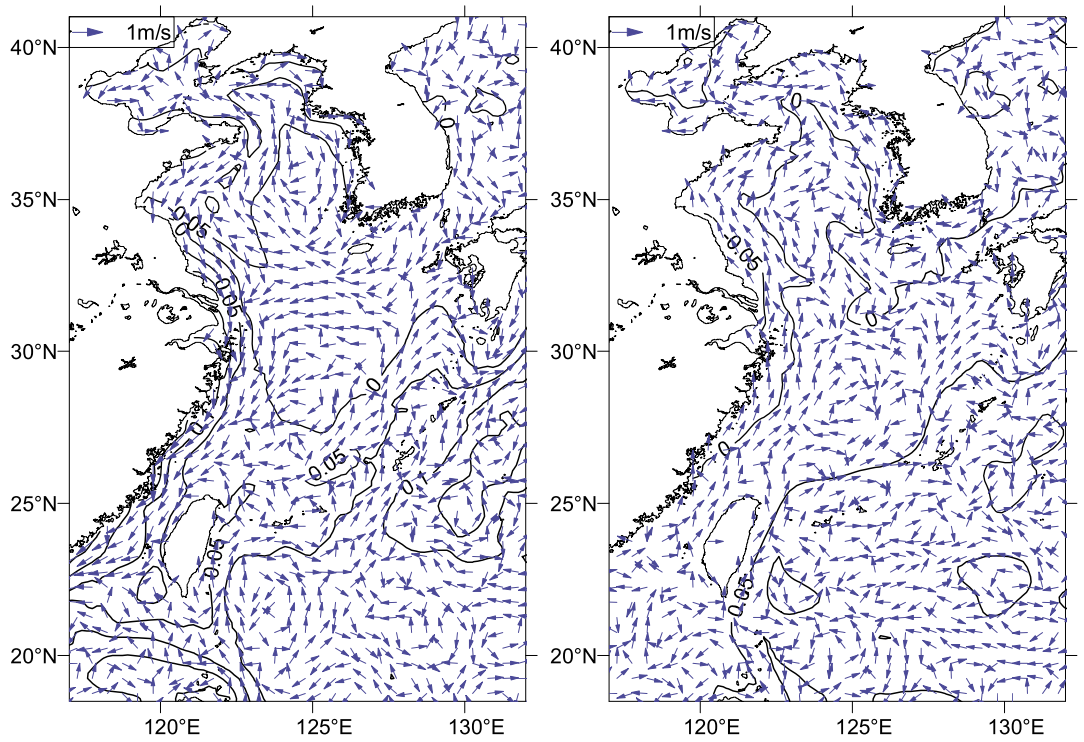

Figure 12. Sea surface height (contours, m) and depth-averaged velocities (arrows, m s^{-1}) of the ECYS in (left) winter (averaged over February in the last model-run year) and (right) summer (averaged over August in the last model-run year) from *sen-exp3*. The contour interval is 0.1 m.

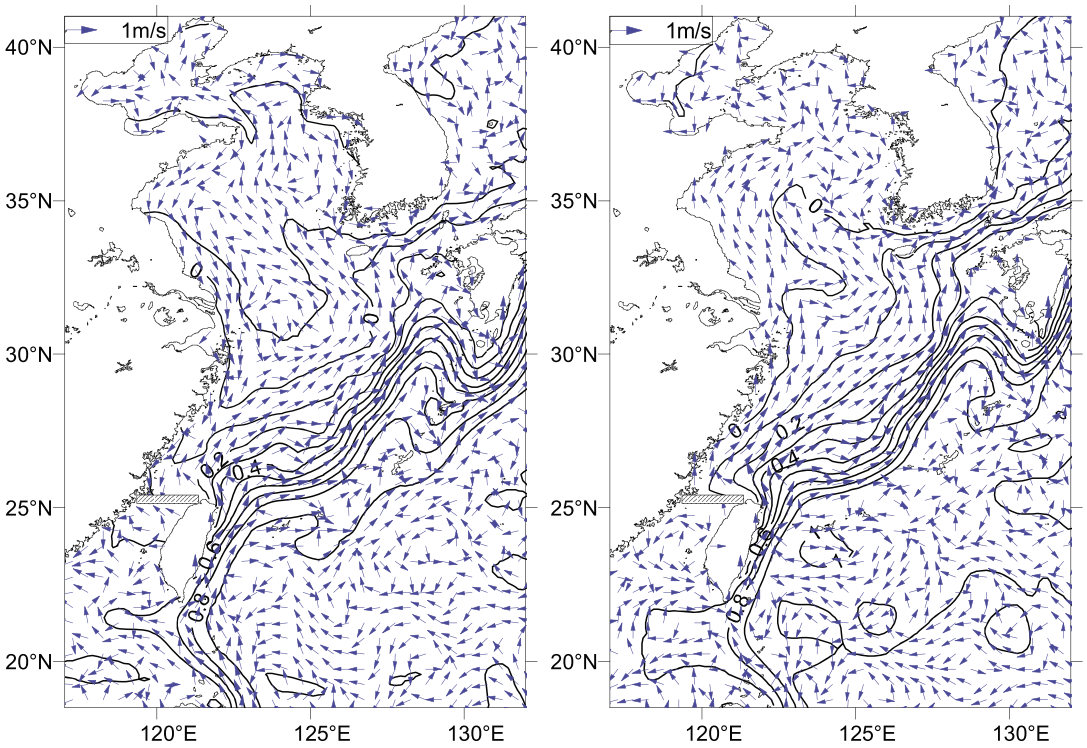

Figure 13. Sea surface height (contours, m) and depth-averaged velocities (arrows, m s^{-1}) of the ECYS in (left) winter (averaged over February in the last model-run year) and (right) summer (averaged over August in the last model-run year) from *sen-exp4*. The contour interval is 0.1 m.

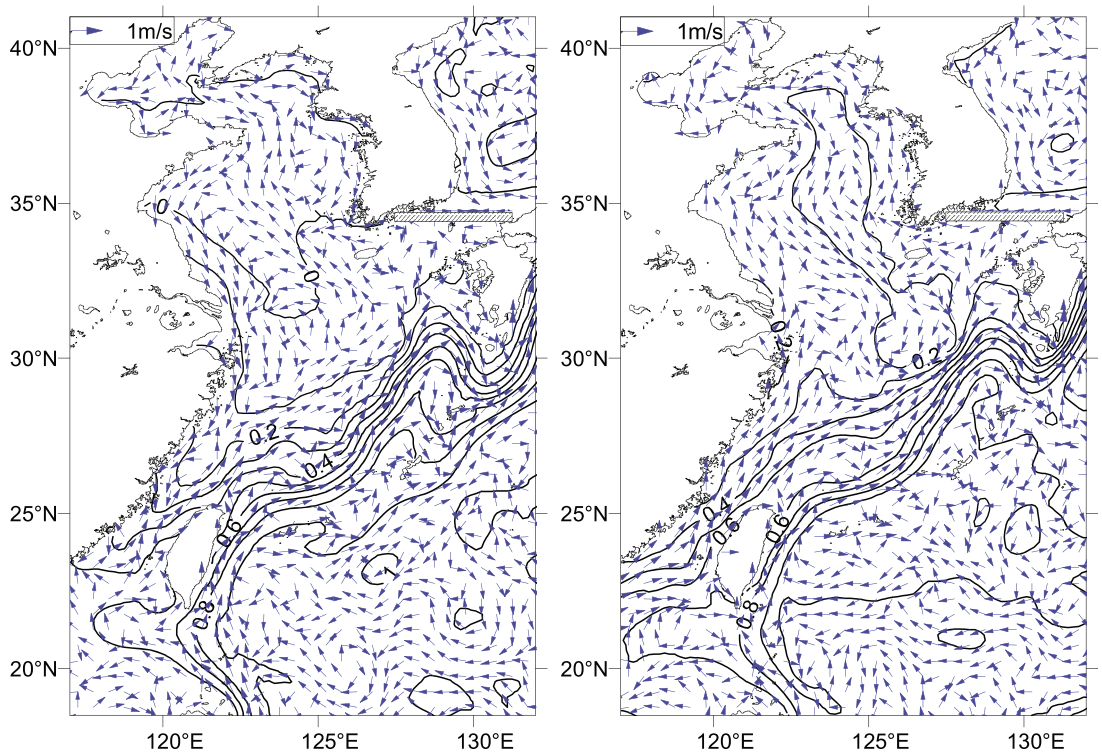

Figure 14. Sea surface height (contours, m) and depth-averaged velocities (arrows, m s^{-1}) of the ECYS in (left) winter (averaged over February in the last model-run year) and (right) summer (averaged over August in the last model-run year) from *sen-exp5*. The contour interval is 0.1 m.

is evidence of its existence as a compensation flow. There are seasonal variations in the circulation of the Yellow Sea in control run: the China Coastal Current changes direction seasonally, but the Korea Coastal Current flows southward all over the year. The result of integration of the two factors will be the existence of a northward YSWC, only with a great weakening in summer. If the local wind stress was removed, the seasonal variation will nearly disappear, which indicates the important effect of the wind stress on it. If the Tsushima Strait was blocked, the Korea Coastal Current will flow in the reverse direction, the YSWC will turn to southward in summer as a result, which demonstrates the indirectly KC effect to the YSWC through the TsWC.

4. Summary and Discussion

[40] In this study, we use a 3-D ocean model to investigate the roles of open-ocean and local forcing mechanisms

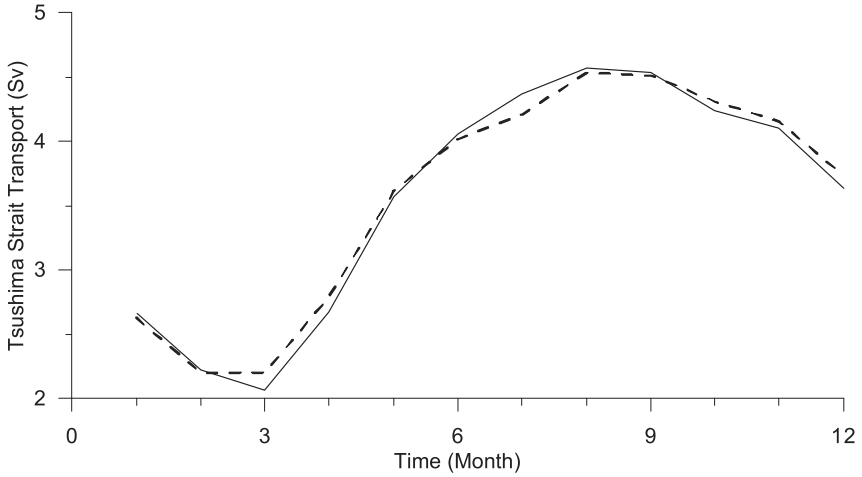

Figure 15. The monthly averaged volume transports (Sv) of the TsWC from *control run* (solid line) and *sen-exp4* (dashed line). The positive transport means northward flow.

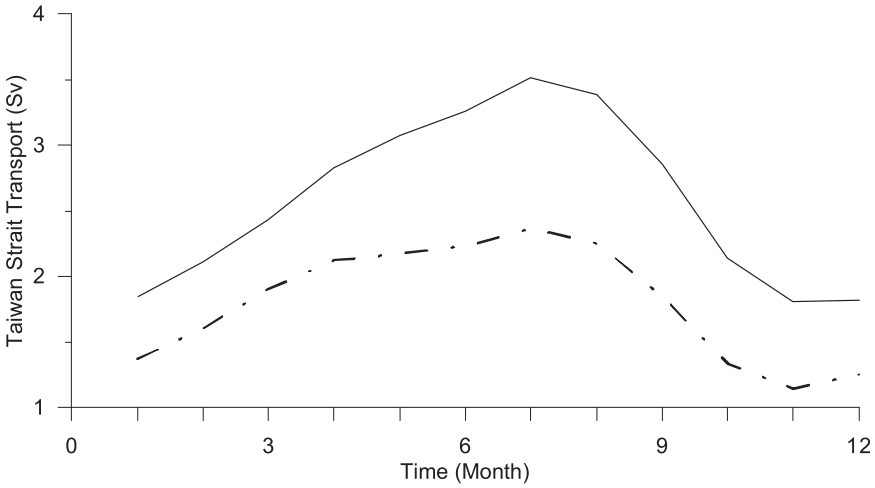

Figure 16. The monthly averaged volume transports (Sv) of the TSC from *control run* (solid line) and *sen-exp5* (dash-dotted line). The positive transport means northward flow.

of major currents in the ECYS. Results from a *control run* and three additional sensitivity experiments are presented to elucidate the relative roles of these two forcing mechanisms. In *sen-exp2* in which the Luzon Strait was blocked, the temperature and salinity fields almost do not change in upper layer over the SCS, except for that there is a little decrease near the Luzon Strait in winter. It is interesting that, the temperature and salinity in the SCS will increase in the depth of 500 ~ 1000 m, and decrease in the depth of more than 1000 m comparing with the *control run*, which may be related the intrusion of water mass through the Luzon Strait. In *sen-exp3* which the KC is removed, the temperature and salinity fields change obviously, especially there are no longer high temperature and salinity tongues along the KC. However, the temperature is still higher in the SCS than that in the ECS all over the year, but the flow along the Taiwan Strait reverses its direction seasonally. It demonstrates that the thermally effect is not the only dominant factor in setting the direction of the flow along the Taiwan Strait. Our results support the finding by *Yang* [2007, 2006] that, on the annual mean basis, the major currents, including TSC, TsWC, YSWC and Korea Coastal Current, are primarily forced by the open ocean through the KC. Large islands, like Taiwan Island and Japan, located on the edge of continental slope, help to facilitate the open-ocean forcing in the shallow coastal seas. Without the KC forcing, local forcing alone would produce a southward flow through the Tsushima Strait, a weak and seasonally reversing flow along the Taiwan Strait, and the absence of the YSWC and Korea Coastal Current. These currents, however, are well simulated by the KC forcing, and are included even in the case where all local forcing is removed.

Table 2. Volume Transports of the China Coastal Current, Yellow Sea Warm Current, and Korea Coastal Current in Both Winter and Summer From *Control Run*, *Sen-exp1*, and *Sen-exp5*[a]

Experiment	Season	CCC	YSWC	KCC
Control run	Winter	−0.15	0.34	−0.19
	Summer	0.06	0.05	−0.11
Sen-exp1	Winter	−0.05	0.12	−0.07
	Summer	−0.05	0.13	−0.08
Sen-exp5	Winter	−0.12	0.23	−0.11
	Summer	0.01	−0.15	0.14

[a]Units are Sv. Positive represents northward, and negative represents southward.

[41] The second goal of our study is to examine the relative role of the open ocean and the local forcing in the seasonal variability that was not previously addressed. It was found that the seasonal variability of the TSC is small when the local wind stress forcing is removed (Figure 10 for the velocity in the region, and the dashed line in Figure 5 for the TSC transport). So we conclude that while the KC is primarily responsible for driving the mean flow through the Taiwan Strait, the local wind stress forcing plays the leading role in modulating the seasonal variability. The annual mean transport of the TSC in the locally forced case (*sen-exp3*, Figure 12 and, dash-dotted line in Figure 5) is negligible compared with that from the *control run*.

[42] The existence of the YSWC as a mean current has been debated in previous studies of regional water mass characteristics [i.e., *Lie et al.*, 2001]. The well-accepted consensus is that the YSWC is robustly developed and penetrates well into the Yellow Sea Trough and even to the Bohai Sea in winter. In summer, however, the existence of the YSWC becomes murkier and the intruding warm water is limited only to the southern trough [e.g., *Lie*, 1986; *Park*, 1986]. The mechanism of this seasonal variation, though well documented, has not been dynamically explained. Our *control run* simulates well this seasonal variation (Figure 3). It is interesting to note that the YSWC is well established in the *sen-exp1* when the local forcing is removed (Figure 10). This indicates that local forcing is not the leading driver for the mean YSWC. However, the current becomes rather steady seasonally, indicating the role of the monsoonal forcing of its seasonal variability. We postulate here that the strengthening of the YSWC in the winter season is due to the pulling effect from the southward flow along the coast of the Chinese mainland. The China Coastal Current is forced by the monsoonal wind and the KC appears to play little role. This is demonstrated in the *sen-exp3* (Figure 12) which

shows that the coastal current and its seasonal variation are similar to the *control run* (Figure 3), even though the KC forcing is removed. During the winter monsoon season, the along-shore wind drives southward flows along the Chinese coast all the way from the Bohai Sea to the SCS and the southwestern coast of Korean Peninsula. To compensate these diverging coastal currents from the Bohai Sea and the northern Yellow Sea, water mass must be drawn to the region. Consequently, the water mass along the Yellow Sea Trough is sucked northward, and this helps to push the YSWC northward against the southward wind.

[43] **Acknowledgments.** This work was supported by the National Basic Research Program of China (2005CB422302), the International Science and Technology Cooperation Program of China (2006DFB21250), the Program of Introducing Talents of Discipline to Universities (B07036), the National Natural Science Foundation of China (41006003), and the U.S. National Science Foundation. NODC WOA01 and ICOADS data are provided by the NOAA/OAR/ESRL PSD, USA, from their Web site at http://www.esrl.noaa.gov/psd/. Special thanks are given to the Laboratory of Marine Science and Numerical Modeling (MASNUM, SOA, China) for providing us with the boundary conditions.

References

Beardsley, R. C., R. Limeburner, and H. Yu (1985), Discharging of the Changjiang (Yangtze River) into the East China Sea, *Cont. Shelf Res.*, *4*, 57–76, doi:10.1016/0278-4343(85)90022-6.

Boyer, T. P., C. Stephens, J. I. Antonov, M. E. Conkright, R. A. Locarnini, T. D. O'Brien, and H. E. Garcia (2002), *World Ocean Atlas 2001* [CD-ROM], vol. 2, *Salinity*, edited by S. Levitus, *NOAA Atlas NESDIS 50*, 165 pp., U.S. Gov. Print. Off., Washington, D.C.

Chen, C.-T. A., and D. D. Sheu (2006), Does the Taiwan Warm Current originate in the Taiwan Strait in wintertime?, *J. Geophys. Res.*, *111*, C04005, doi:10.1029/2005JC003281.

Chen, C.-T. A., S. Jan, T.-H. Huang, and Y.-H. Tseng (2010), Spring of no Kuroshio intrusion in the southern Taiwan Strait, *J. Geophys. Res.*, *115*, C08011, doi:10.1029/2009JC005804.

Chu, P. C., and R. Li (2000), South China Sea isopycnal-surface circulation, *J. Phys. Oceanogr.*, *30*, 2419–2438, doi:10.1175/1520-0485(2000)030<2419:SCSISC>2.0.CO;2.

Chuang, W. S. (1985), Dynamics of subtida1 flow in the Taiwan Strait, *J. Oceanogr.*, *41*, 65–72.

Chuang, W. S. (1986), A note on the driving mechanism of the current in the Taiwan Strait, *J. Oceanogr.*, *42*, 355–361.

Fang, G. (1995), The structure of the Taiwan-Tsushima-Tsugaru current system and its relation to the Kuroshio (in Chinese), *Mar. Sci.*, *4*, 43–48.

Fang, G., and B. Zhao (1988), A note on the main forcing of the northeastward flowing current off the southeast China coast, *Prog. Oceanogr.*, *21*, 363–372, doi:10.1016/0079-6611(88)90014-6.

Fang, G., B. Zhao, and Y. Zhu (1991), Water volume transports through the Taiwan Strait and the East China Sea measured with current meters, in *Oceanography of Asian Marginal Seas*, edited by K. Takano, pp. 345–358, doi:10.1016/S0422-9894(08)70107-7, Elsevier, Amsterdam.

Fang, G., B. Zhao, and Y. Zhu (1992), A preliminary study on the Taiwan-Tsushima-Tsugaru Warm Current System and its dynamic mechanism (in Chinese), in *Selected Papers of Symposium on Ocean Circulation*, edited by Q. Zeng et al., pp. 13–27, China Ocean, Beijing.

Fang, G., et al. (1998), A survey of studies on the South China Sea upper ocean circulation, *Acta Oceanogr. Taiwan.*, *37*(1), 1–16.

Fang, G., Z. Wei, B. Cui, K. Wang, Y. Fang, and W. Li (2002), Transportation of water, heat and salt in China Sea: Results of global changing grid model (in Chinese), *Sci. China Ser. D*, *32*(12), 969–977.

Fang, G., D. Susanto, I. Soesilo, Q. Zheng, F. Qiao, and Z. Wei (2005), A note on the South China Sea shallow interocean circulation, *Adv. Atmos. Sci.*, *22*, 946–954, doi:10.1007/BF02918693.

Guan, B. (1981), Analysis of the variations of volume transports of the Kuroshio in the East China Sea: Proceedings of the Japan-China Symposium on Physical Oceanography and Marine Engineering in the East China Sea, in *Special Report of Institute of Ocean Research*, pp. 118–137, Tokai Univ., Shimizu, Japan.

Guan, B. (1986), Evidence for a counter-wind current in winter off the southeast coast of China, *Chin. J. Oceanol. Limnol.*, *4*(4), 319–332, doi:10.1007/BF02845279.

Guan, B., and G. Fang (2006), Winter counter-wind currents off the southeastern China coast: A review, *J. Oceanogr.*, *62*, 1–24, doi:10.1007/s10872-006-0028-8.

Guo, X. (1999), On the volume transport through the Taiwan Strait, paper presented at 10th Pacific Asian Marginal Seas/Japan and East China Study Workshop, Kagoshima Univ., Kagoshima, Japan.

Guo, X., Y. Miyazawa, and T. Yamagata (2006), The Kuroshio onshore intrusion along the shelf break of the East China Sea: The origin of the Tsushima Warm Current, *J. Phys. Oceanogr.*, *36*, 2205–2231, doi:10.1175/JPO2976.1.

Ichikawa, H., and R. C. Beardsley (2002), The current system in the Yellow Sea and East China Sea, *J. Oceanogr.*, *58*, 77–92, doi:10.1023/A:1015876701363.

Isobe, A. (1999), On the origin of the Tsushima Warm Current and its seasonality, *Cont. Shelf Res.*, *19*, 117–133, doi:10.1016/S0278-4343(98)00065-X.

Isobe, A. (2000), Two-layer model on the branching of the Kuroshio southwest of Kyushu, *J. Phys. Oceanogr.*, *30*, 2461–2476, doi:10.1175/1520-0485(2000)030<2461:TLMOTB>2.0.CO;2.

Isobe, A. (2008), Recent advances in ocean-circulation research on the Yellow Sea and East China Sea shelves, *J. Oceanogr.*, *64*, 569–584, doi:10.1007/s10872-008-0048-7.

Johns, W. E., T. N. Lee, D. Zhang, R. Zantopp, C. T. Liu, and Y. Yang (2001), The Kuroshio east of Taiwan: Moored transport observations from the WOCE PCM-1 array, *J. Phys. Oceanogr.*, *31*, 1031–1053, doi:10.1175/1520-0485(2001)031<1031:TKEOTM>2.0.CO;2.

Li, R., and Q. Zeng (1994), A numerical simulation of the winter-time current system in the China Sea and adjacent areas, *Sci. China Ser. B*, *37*(6), 710–722.

Li, R., Q. Zeng, Z. Ji, and D. Guo (1992), Numerical simulation of a northeastward flowing current from area off the Eastern Hainan Island to Tsugaru/Soya Strait, *Mer*, *30*, 229–238.

Li, R., Q. Zeng, Z. Gan, and W. Wang (1993), Numerical simulation of the South China Sea Warm Current and the Taiwan Strait flow in winter, *Prog. Nat. Sci.*, *3*(2), 123–129.

Liang, W. D., T. Y. Tang, Y. J. Yang, M. T. Ko, and W. S. Chuang (2003), Upper-ocean currents around Taiwan, *Deep Sea Res., Part II*, *50*, 1085–1105, doi:10.1016/S0967-0645(03)00011-0.

Lie, H.-J. (1986), Summertime hydrographic features in the southeastern Hwanghae, *Prog. Oceanogr.*, *17*, 229–242, doi:10.1016/0079-6611(86)90046-7.

Lie, H.-J., and C.-H. Cho (1994), On the origin of the Tsushima Warm Current, *J. Geophys. Res.*, *99*(C12), 25,081–25,091, doi:10.1029/94JC02425.

Lie, H.-J., C.-H. Cho, and A. Kaneko (1998), On the branching of the Kuroshio and the formation of slope countercurrent in the East China Sea, paper presented at China-Japan Joint Symposium on Cooperative Study of Subtropical Circulation System, Fish. Agency Jpn., Nagasaki, Japan.

Lie, H.-J., C.-H. Cho, J.-H. Lee, S. Lee, Y. Tang, and E. Zou (2001), Does the Yellow Sea Warm Current really exist as a persistent mean flow?, *J. Geophys. Res.*, *106*(C10), 22,199–22,210, doi:10.1029/2000JC000629.

Lim, D.-B. (1971), On the origin of the Tsushima Warm Current Water, *J. Oceanogr. Soc. Korea*, *22*, 85–91.

Mask, A. C., and J. J. O'Brien (1998), Wind-driven effects on the Yellow Sea Warm Current, *J. Geophys. Res.*, *103*(C13), 30,713–30,729, doi:10.1029/1998JC900007.

Mellor, G. L., and T. Yamada (1982), Development of a turbulence closure model for geophysical fluid problems, *Rev. Geophys.*, *20*(4), 851–875, doi:10.1029/RG020i004p00851.

Metzger, E. J., and H. E. Hurlburt (1996), Coupled dynamics of the south China Sea, the Sulu Sea, and the Pacific Ocean, *J. Geophys. Res.*, *101*(C5), 12,331–12,352, doi:10.1029/95JC03861.

Minato, S., and R. Kimura (1980), Volume transport of the western boundary current penetrating into a marginal sea, *J. Oceanogr.*, *36*, 185–195.

National Oceanic and Atmospheric Administration (NOAA) (1988), Digital relief of the surface of the Earth, *Data Announce. 88-MGG-02*, Natl. Geophys. Data Cent., Boulder, Colo.

Nitani, H. (1972), Beginning of the Kuroshio, in *Kuroshio: Its Physical Aspects*, edited by H. Stommel and K. Yoshida, pp. 129–163, Univ. of Tokyo Press, Tokyo.

Park, Y.-H. (1986), Water characteristics and movements of the Yellow Sea Warm Current in summer, *Prog. Oceanogr.*, *17*, 243–254, doi:10.1016/0079-6611(86)90047-9.

Pedlosky, J., L. J. Pratt, M. A. Spall, and K. R. Helfrich (1997), Circulation around islands and ridges, *J. Mar. Res.*, *55*, 1199–1251, doi:10.1357/0022240973224085.

Qiao, F., Y. Yuan, Y. Yang, Q. Zheng, C. Xia, and J. Ma (2004), Wave-induced mixing in the upper ocean: Distribution and application to a

global ocean circulation model, *Geophys. Res. Lett.*, *31*, L11303, doi:10.1029/2004GL019824.

Qiu, B., and R. Lukas (1996), Seasonal and interannual variability of the North Equatorial Current, Mindanao Current, and the Kuroshio along the Pacific western boundary, *J. Geophys. Res.*, *101*(C5), 12,315–12,330, doi:10.1029/95JC03204.

Qu, T. (2000), Upper-layer circulation in the South China Sea, *J. Phys. Oceanogr.*, *30*, 1450–1460, doi:10.1175/1520-0485(2000)030<1450:ULCITS>2.0.CO;2.

Qu, T., and R. Lukas (2003), The bifurcation of the North Equatorial Current in the Pacific, *J. Phys. Oceanogr.*, *33*, 5–18, doi:10.1175/1520-0485(2003)033<0005:TBOTNE>2.0.CO;2.

Qu, T., H. Mitsudera, and T. Yamagata (1998), On the western boundary currents in the Philippine Sea, *J. Geophys. Res.*, *103*(C4), 7537–7548, doi:10.1029/98JC00263.

Qu, T., Y. Du, G. Meyers, A. Ishida, and D. Wang (2005), Connecting the tropical Pacific with Indian Ocean through South China Sea, *Geophys. Res. Lett.*, *32*, L24609, doi:10.1029/2005GL024698.

Qu, T., Y. Du, and H. Sasaki (2006), South China Sea throughflow: A heat and freshwater conveyor, *Geophys. Res. Lett.*, *33*, L23617, doi:10.1029/2006GL028350.

Qu, T., Y. T. Song, and T. Yamagata (2009), An introduction to the South China Sea throughflow: Its dynamics, variability, and application for climate, *Dyn. Atmos. Oceans*, *47*, 3–14, doi:10.1016/j.dynatmoce.2008.05.001.

Sawara, T., and Y. Hanzawa (1979), Distribution of water type in the East China Sea, *Umi Sora*, *54*, 135–148.

Stephens, C., J. I. Antonov, T. P. Boyer, M. E. Conkright, R. A. Locarnini, T. D. O'Brien, and H. E. Garcia (2002), *World Ocean Atlas 2001* [CD-ROM], vol. 1, *Temperature*, edited by S. Levitus, *NOAA Atlas NESDIS 49*, 167 pp., U.S. Gov. Print. Off., Washington, D.C.

Su, J. (2001), A review of circulation dynamics of the coastal oceans near China (in Chinese), *Acta Oceanol. Sin.*, *23*(4), 1–16.

Su, J., and W. Wang (1987), On the sources of the Taiwan Warm Current from the South China Sea, *Chin. J. Oceanol. Limnol.*, *5*(4), 299–308, doi:10.1007/BF02843812.

Su, J., Y. Pan, and X. Liang (1994), Kuroshio intrusion and Taiwan Warm Current, in *Oceanology of China Seas*, edited by D. Zhou, Y. Liang, and C. Zeng, pp. 59–70, Kluwer Acad., Dordrecht, Netherlands.

Susanto, R. D., and A. L. Gordon (2005), Velocity and transport of the Makassar Strait throughflow, *J. Geophys. Res.*, *110*, C01005, doi:10.1029/2004JC002425.

Takikawa, T., J.-H. Yoon, and K.-D. Cho (2005), The Tsushima Warm Current through Tsushima Straits estimated from ferryboat ADCP data, *J. Phys. Oceanogr.*, *35*, 1154–1168, doi:10.1175/JPO2742.1.

Teague, W. J., G. A. Jacobs, H. T. Perkins, J. W. Book, K.-I. Chang, and M.-S. Suk (2002), Low-frequency current observations in the Korea/Tsushima Strait, *J. Phys. Oceanogr.*, *32*, 1621–1641, doi:10.1175/1520-0485(2002)032<1621:LFCOIT>2.0.CO;2.

Teague, W. J., G. A. Jacobs, D. S. Ko, T. Y. Tang, K.-I. Chang, and M.-S. Suk (2003), Connectivity of the Taiwan, Cheju, and Korea straits, *Cont. Shelf Res.*, *23*, 63–77, doi:10.1016/S0278-4343(02)00150-4.

Tomczak, M., and J. S. Godfrey (1994), *Regional Oceanography: An Introduction*, 442 pp., Pergamon, Oxford, U.K.

Tozuka, T., T. Qu, and T. Yamagata (2007), Effect of South China Sea throughflow on the Makassar Strait throughflow, *Geophys. Res. Lett.*, *34*, L12612, doi:10.1029/2007GL030420.

Tozuka, T., T. Qu, Y. Masumoto, and T. Yamagata (2009), Impacts of the South China Sea Throughflow on seasonal and interannual variations of the Indonesian Throughflow, *Dyn. Atmos. Oceans*, *47*, 73–85, doi:10.1016/j.dynatmoce.2008.09.001.

Wang, D., Q. Liu, R. Huang, Y. Du, and T. Qu (2006), Interannual variability of the South China Sea throughflow inferred from wind data and an ocean data assimilation product, *Geophys. Res. Lett.*, *33*, L14605, doi:10.1029/2006GL026316.

Wang, Y. H., S. Jan, and D. P. Wang (2003), Transports and tidal current estimates in the Taiwan Strait from shipboard ADCP observations (1999–2001), *Estuarine Coastal Shelf Sci.*, *57*, 193–199, doi:10.1016/S0272-7714(02)00344-X.

Worley, S. J., S. D. Woodruff, R. W. Reynolds, S. J. Lubker, and N. Lott (2005), ICOADS release 2.1 data and products, *Int. J. Climatol.*, *25*, 823–842, doi:10.1002/joc.1166.

Xia, C., F. Qiao, Q. Zhang, and Y. Yuan (2004), Numerical modelling of the quasi-global ocean circulation based on POM, *J. Hydrodynam.*, *15*(5), 537–543.

Yang, J. (2006), The Kuroshio Forcing of the East Asian Marginal Seas, *Eos Trans. AGU*, *87*(36), West. Pac. Geophys. Meet. Suppl., Abstract OS42A.

Yang, J. (2007), An oceanic current against the wind: How does Taiwan Island steer warm water into the East China Sea, *J. Phys. Oceanogr.*, *37*, 2563–2569, doi:10.1175/JPO3134.1.

Yaremchuk, M., and T. Qu (2004), Seasonal variability of the large-scale currents near the coast of the Philippines, *J. Phys. Oceanogr.*, *34*, 844–855, doi:10.1175/1520-0485(2004)034<0844:SVOTLC>2.0.CO;2.

Yaremchuk, M., J. McCreary, Z. Yu, and R. Furue (2009), The South China Sea throughflow retrieved from climatological data, *J. Phys. Oceanogr.*, *39*, 753–767, doi:10.1175/2008JPO3955.1.

Yu, Z., S. Shen, J. P. McCreary, M. Yaremchuk, and R. Furue (2007), South China Sea throughflow as evidenced by satellite images and numerical experiments, *Geophys. Res. Lett.*, *34*, L01601, doi:10.1029/2006GL028103.

Zhu, J., C. Chen, P. Ding, C. Li, and H. Lin (2004), Does the Taiwan warm current exist in winter?, *Geophys. Res. Lett.*, *31*, L12302, doi:10.1029/2004GL019997.

X. Ju, The First Institute of Oceanography, State Oceanic Administration, Qingdao, 266061, China.

X. Lin, C. Ma, and D. Wu, Physical Oceanography Laboratory, Ocean University of China, 238 Songling Rd., Qingdao, 266100, China. (machao@ouc.edu.cn)

J. Yang, Department of Physical Oceanography, Woods Hole Oceanographic Institution, Woods Hole, MA 02543, USA.